ELSEVIER

Tectonophysics 321 (2000) 189–218

TECTONOPHYSICS

www.elsevier.com/locate/tecto

Active faults and evolving strike-slip basins in the Marmara Sea, northwest Turkey: a multichannel seismic reflection study

A.I. Okay [a,*], A. Kaşlılar-Özcan [b], C. İmren [b], A. Boztepe-Güney [b], E. Demirbağ [b], İ. Kuşçu [c]

[a] *Avrasya Yerbilimleri Enstitüsü, İstanbul Teknik Üniversitesi, Ayazağa 80626, Istanbul, Turkey*
[b] *Jeofizik Mühendisliği Bölümü, Maden Fakültesi, İstanbul Teknik Üniversitesi, Ayazağa 80626, Istanbul, Turkey*
[c] *Jeoloji Etüdleri Dairesi, Maden Tetkik ve Arama Genel Müdürlüğü, Ankara, Turkey*

Received 6 September 1999; accepted for publication 24 January 2000

Abstract

The North Anatolian Fault is a 1200-km-long transform fault forming the boundary between the Anatolian and Eurasian plates. Near its western end it strikes through the Marmara Sea, and is responsible for the creation of three deep marine depressions. The North Anatolian Fault system and the linked basins in the eastern Marmara Sea were studied using newly acquired multi-channel seismic reflection data. In the Marmara Sea the North Anatolian Fault consists of a main strand and a few subsidiary branches. The main strand is made up of the Ganos (15 km long), Central Marmara (105 km) and North Boundary (45 km) fault segments. The North Boundary Fault joins in the east to the İzmit segment, which was ruptured during the M_S 7.4 earthquake on 17.8.1999. The North Boundary Fault is highly oblique to the regional displacement vector, which results in the generation of a symmetrical fault-wedge basin. This Çınarcık Basin is a wedge-shaped deep marine depression south of İstanbul. It is about 50 km long, up to 20 km wide and 1250 m deep, and is filled with Pliocene to Quaternary sediments, over 3 km thick. The North Boundary Fault joins in the west to the transpressional Central Marmara Fault. Around the restraining segment boundary the syntransform sediments are being deformed into a large anticlinorium. The Çınarcık Basin started to form when the westward-propagating North Anatolian Fault intersected a northwest-trending pre-existing fault zone during the Pliocene and bifurcated into NW- and SW-trending segments, forming a transform–transform–transform-type triple junction. Dextral strike-slip movement along the arms of the triple junction led to the development of the Çınarcık Basin. The present fault geometry in the Marmara region was achieved later during the mid-Pliocene following the termination of the triple junction geometry. South of the main North Anatolian Fault system there is a second active strike-slip fault in the Marmara Sea made up of several segments. A highly asymmetrical fault-bend basin, comprising Pliocene–Quaternary sediments over 2.5 km thick, is forming along a releasing fault segment of this South Boundary Fault system.

Keywords: basin formation; Marmara Sea; North Anatolian Fault; seismic data; strike-slip fault; Turkey

* Corresponding author. Tel.: +90-212-285-62-08; fax: +90-212-285-62-10.
E-mail address: okay@itu.edu.tr (A.I. Okay)

0040-1951/00/$ - see front matter
PII: S0040-1951(00)00046-9

1. Introduction

The North Anatolian Fault is a transform fault forming part of the boundary between the Eurasian and African–Arabian plates (Fig. 1). The Anatolian plate, caught between the converging Eurasian and Arabian plates, escapes westwards along the dextral North Anatolian and sinistral East Anatolian faults into the north–south-extending Aegea (McKenzie, 1972). The North Anatolian Fault nucleated in the eastern Anatolia during the Late Miocene and propagated westwards reaching the Marmara region sometime during the Pliocene (e.g. Şengör, 1979; Suzanne et al., 1990; Barka, 1992). In the Marmara region, the North Anatolian Fault shows two features not observed in the rest of its 1200-km-long fault zone. There are several deep marine strike-slip basins, which constitute part of the Marmara Sea, and on land there are NW- and SW-trending major dextral strike-slip fault zones with no apparent relation to the west-trending active branch of the North Anatolian Fault (Fig. 2). We have studied strike-slip basins in the eastern Marmara Sea with the aim of understanding the mechanism of the basin formation, mechanics and timing of the westward propagation of the North Anatolian Fault, and its relation to the discordant NW- and SW-trending post-Miocene strike-slip fault zones. Our main tool during this study has been 832 km long multichannel seismic sections, run across the eastern Marmara Sea by Mineral Research and

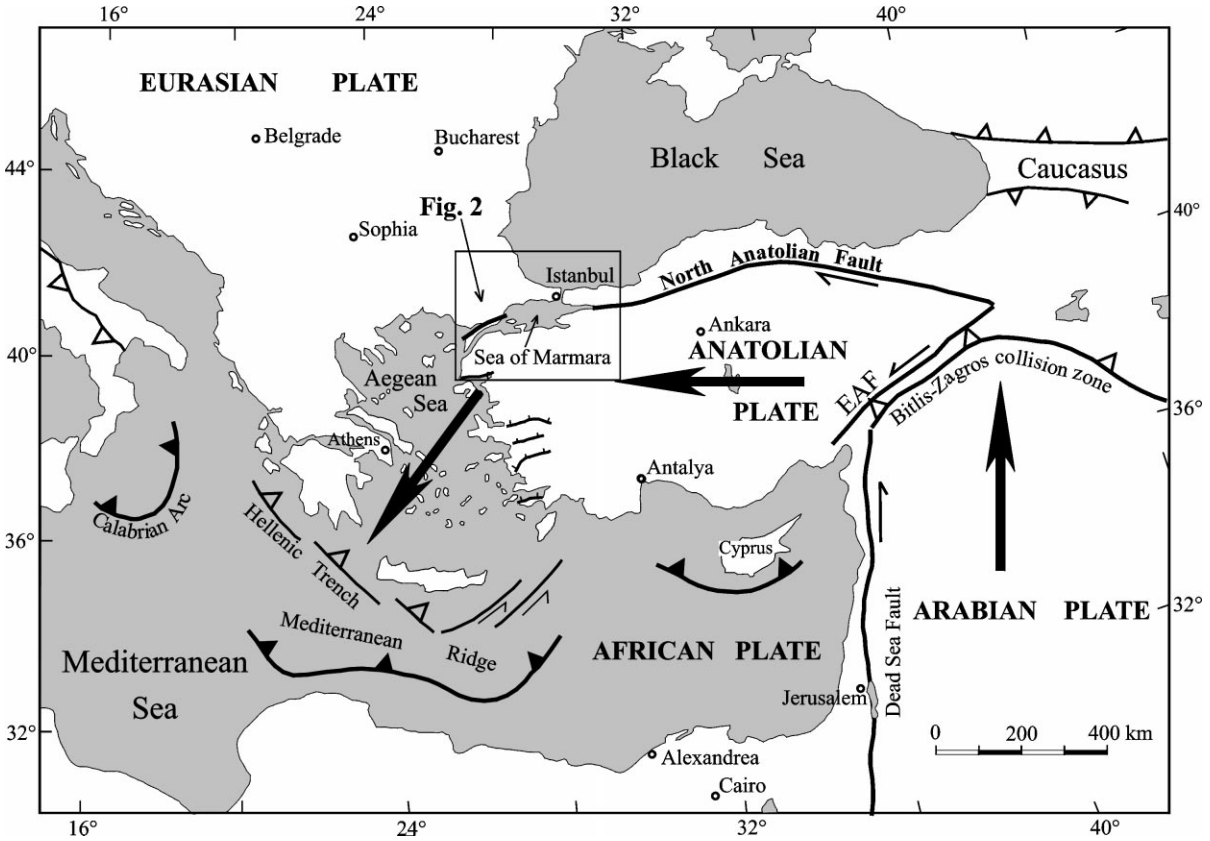

Fig. 1. Active tectonic map of the eastern Mediterranean region showing the geological setting of the Marmara Sea. Lines with filled triangles show active subduction zones, lines with open triangles are active thrust faults at continental collision zones, and lines with tick marks are normal faults. The large solid arrows indicate the sense of motion of the lithospheric plates. EAF: East Anatolian Fault.

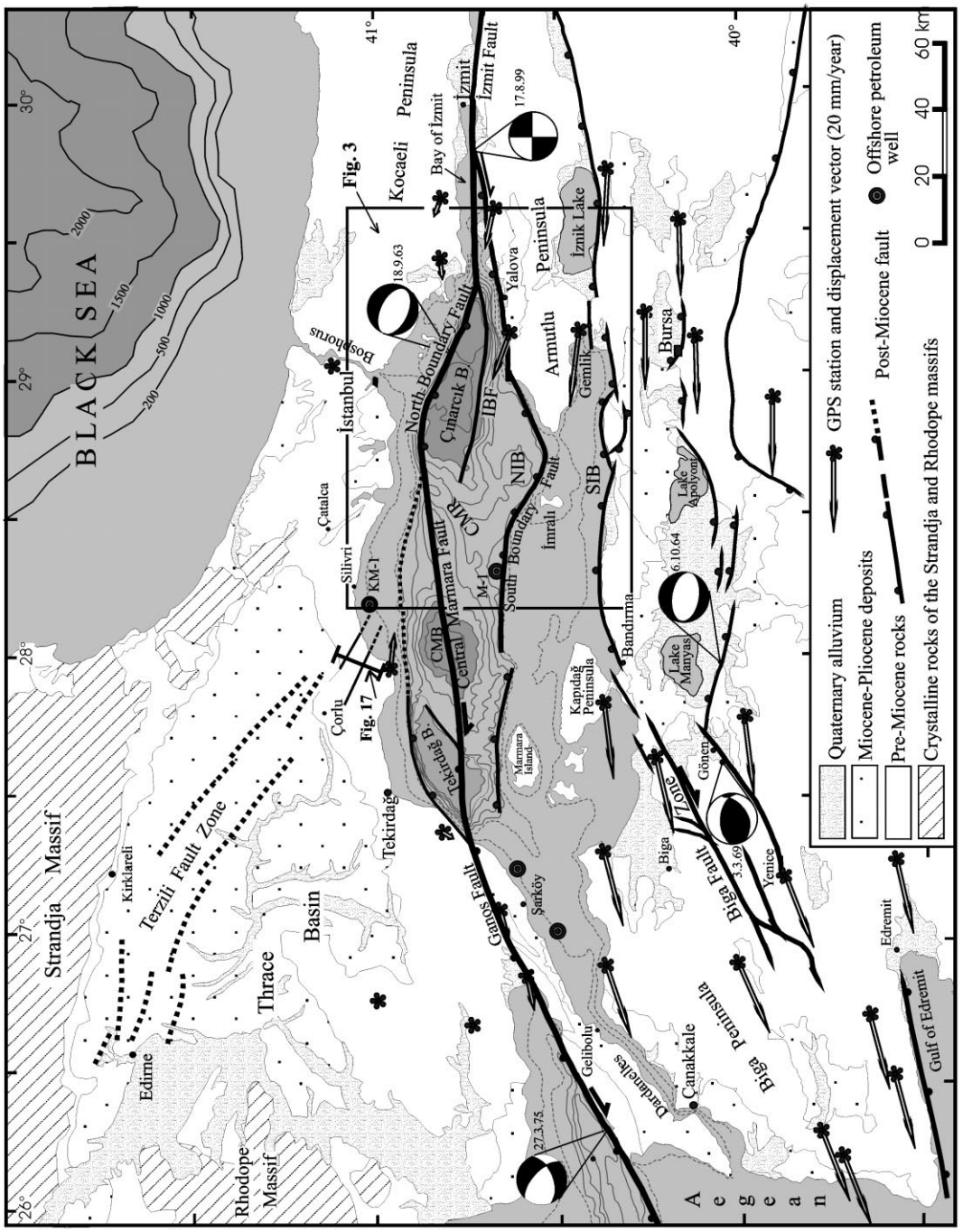

Fig. 2. Active tectonic map of the Marmara region. For the location, see Fig. 1. The map is compiled from MTA (1964), Perinçek (1991), Şaroğlu et al. (1992), Okay et al. (1999). Faults shown cut Miocene or younger sediments. The bathymetric contours in the Marmara Sea, drawn at 50, 100, then at every 200 m, are slightly modified from Smith et al. (1995). The fault plane solutions of the major earthquakes ($M_S > 5$) are from Taymaz et al. (1991) and USGS (1999). The stars and arrows respectively indicate global positioning system (GPS) station localities and displacement vectors with respect to a fixed station in İstanbul (Straub et al. 1997). CMR: Central Marmara Ridge; CMB: Central Marmara Basin; IBF: Inner Boundary Fault; NIB: North İmralı Basin; SIB: South İmralı Basin; km-1: Kuzey Marmara-1 well; M-1: Marmara-1 well.

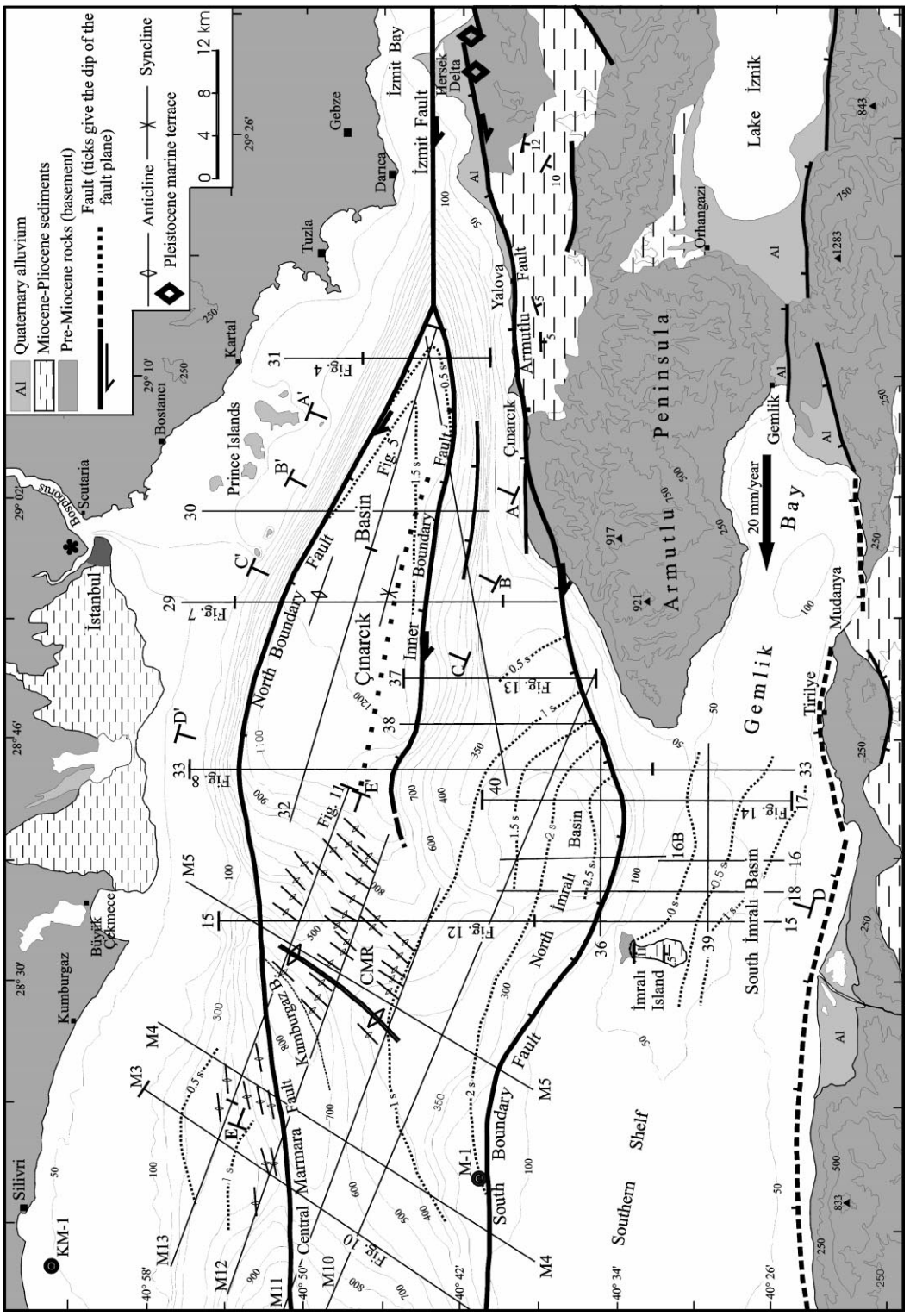

Fig. 3. Tectonic map of the eastern Marmara Sea. For the location, see Fig. 2. The map shows the major active offshore faults as mapped from seismic sections, the thickness (in seconds) of the syntransform sediments in the Çınarcık, North and South İmralı basins (dotted lines), and the location of the multichannel seismic reflection lines obtained on board the Maden Tetkik ve Arama Enstitüsü (MTA) Sismik-1 during 1997 and 1999. The sections of the seismic lines shown in figures are bracketed by dashes. The bathymetry in metres is compiled from Seyir, Hidrografi ve Oşinografi Dairesi Başkanlığı (1983, 1987, 1989), Güneysu (1998) and from the seismic lines. The solid arrow indicates the regional displacement vector.

Exploration General Directorate (MTA, Maden Tetkik ve Arama) research ship Sismik-1 in 1997 and 1999. Seismic reflection profiles have been widely used in the identification and mapping of strike-slip faults in marine environments (e.g. Harding, 1985; Roussos and Lyssimachou, 1991; Rohr and Dietrich, 1992). The seismic sections in the Marmara Sea delineate accurately the active faults, as well as the geometry of the strike-slip basins. A further aim of the study has been to map the active faults in the Marmara Sea, which lie within 20 km of the metropolitan area of İstanbul and form a major threat to a population of over 10 million people and to the industrial heartland of Turkey. The İstanbul region has been repeatedly affected by damaging earthquakes during the historical period (see Ambraseys and Finkel, 1991, 1995) and recently in a 7.4 M_S earthquake in 17.8.1999, which resulted in the deaths of over 17 000 people with a major loss to the economy. Previous mapping of active faults in the eastern Marmara Sea has been based largely on bathymetry (Pfannenstiel, 1944; Barka and Kadinsky-Cade, 1988) or on single-channel seismic reflection profiles (Ergün and Özel, 1995; Wong et al., 1995). This study provides the first multi-channel reflection profiles from the eastern Marmara Sea.

GPS measurements and earthquake seismicity indicate that the Anatolian plate is moving westward as a largely coherent block up to the Aegean region, where it starts extending north–south along several widely spaced west-trending normal faults (McKenzie, 1972; Reilinger et al., 1997; Fig. 1). The Marmara Sea is located in this transition zone from coherent westward displacement of the Anatolian plate to the diffuse north–south extension. A local GPS network around the Marmara Sea has shown that the Anatolian Plate south of the Marmara Sea is moving westward at a rate of 2 cm/year (Fig. 2, Straub and Kahle, 1995; Straub et al., 1997). The North Anatolian Fault enters the Marmara Sea through the İzmit Bay and emerges in Thrace on the other side forming the Ganos fault segment (Fig. 2). The Ganos fault extends westward following the steep northern submarine margin of the Gallipoli Peninsula into the North Aegean trough.

2. Bathymetric and structural features of the Marmara Sea

The Marmara Sea consists essentially of three submarine depressions, over 1100 m in depth, aligned to the west-trend of the North Anatolian Fault (Fig. 2). Submarine ridges rising several hundreds of meters above the floors of the neighbouring basins separate these depressions. They trend northeast obliquely to the main west-trend of the North Anatolian Fault. In the eastern Marmara Sea, the Central Marmara Ridge separates the Central Marmara Basin in the west from the Çınarcık Basin in the east. The Çınarcık Basin, located south of İstanbul, is bordered in the north by a narrow shelf, and in the south by a wide and deep shelf area, which forms the location of another evolving transtensional basin, the North İmralı Basin. South of the deep shelf there is an equally wide shelf area, where the island of İmralı is located (Fig. 2). Steep submarine slopes, which mark the location of the active faults, separate these bathymetric features.

Several seismic reflection lines were run across the eastern Marmara Sea during the Marmara leg of the Maden Tetkik ve Arama Enstitüsü (MTA) Sismik-1 in 1997 and 1999 (Fig. 3). Continuous positioning of the vessel was maintained by a differential geographical positioning system (DGPS) with a reference station erected near Tekirdağ. The system has an accuracy of better than 5 m.

The data were collected by using an air gun source array of 1380 in^3 and a 96-channel streamer. The receiver group interval was 12.5 m, and offsets were 50 m. The recording length, sampling, and shooting intervals were 8 s, 2 ms, and 50 m respectively. These data collection parameters provided maximum 12-fold reflection seismic data, necessary vertical resolution to distinguish the stratigraphy, and horizontal resolution to trace the faults.

Data processing was done at the Data Processing Laboratory of the Department of Geophysics at the İstanbul Technical University (İTÜ). A conventional seismic data processing stream was applied to the data to obtain the interpreted sections displayed in this article. The processing stream was as follows: data reformat-

ting, in-line field geometry definition, trace editing, spherical divergence correction, frequency filtering, sorting, velocity analysis, dynamic correction, muting, stacking, frequency filtering, time domain migration, frequency filtering, and finally automatic gain correction. The structural and stratigraphic information from the seismic sections were transferred to 1:100 000 scale maps, which formed the basis of our interpretations. In converting two-way travel time to depth we used an average velocity of 2000 m/s for the Pliocene–Quaternary basinal sediments.

2.1. The northern shelf and geology of the adjoining land areas

In the eastern Marmara Sea, the northern shelf has a width of 7 to 13 km. The shelf narrows eastwards towards the entrance of the İzmit Bay (Figs. 2 and 3). The shelf edge is a well-marked bathymetric feature at a depth of ~ -110 m. The shelf west of Çatalca is bordered in the north by the Thrace Basin filled with Eocene to Lower Miocene clastic sedimentary rocks up to 9 km thick (e.g. Kopp et al., 1969; Turgut et al., 1991; Görür and Okay, 1996). The clastic rocks of the Thrace Basin also extend to the Thracian shelf area, as revealed by the offshore well data. The Kuzey Marmara-1 petroleum well (KM-1) drilled southwest of Silivri (Fig. 2) has cut 1100 m Eocene–Lower Miocene sandstones overlain by less than 20 m of Quaternary marine strata (Ergün and Özel, 1995). The coastal region between Çatalca and the Bosphorus consists of Upper Miocene continental to lagoonal sedimentary rocks, less than 150 m thick, which lie unconformably over the Middle Eocene limestones and Palaeozoic sedimentary rocks (Fig. 3). The Palaeozoic rocks extend to the east of Bosphorus forming a thick sedimentary sequence of Ordovician to Carboniferous age (e.g. Görür et al., 1997a). The Prince islands, which lie on the northern shelf (Fig. 3), consist mainly of Ordovician quartzites (Ketin, 1953). These Palaeozoic sedimentary rocks must also extend south to the shelf area.

2.2. The Çınarcık Basin and the enclosing faults

The Çınarcık Basin is a wedge-shaped depression ~ 50 km long and 20 km at its widest extent in the west, and with a surface area of 545 km^2 (Fig. 3). The basin floor is remarkably flat and featureless and most of it lies at a depth of -1270 to -1150 m. The deepest part of the basin, at -1289 m (Seyir, Hidrografi ve Oşinografi Dairesi Başkanlığı, 1989), is in the east and the basin floor rises very gently towards the west (average dip 0.2° or 3.5 m/km). In the west the Çınarcık Basin is bordered by the Central Marmara Ridge, and in the north and south by steeply dipping submarine slopes.

The northern submarine slope is a distinct bathymetric feature, which can be traced in the Marmara Sea for 160 km as a continuous, steep submarine escarpment, separating the northern shelf from the deep basins in the south (Fig. 2). It corresponds to a major fault, named the North Boundary Fault by Wong et al. (1995). North of the Çınarcık Basin, the northern slope is ~ 3 km wide with an average dip of 17°. The Çınarcık basin is bounded in the south by the inner Marmara slope, which is 4 to 6 km wide and dips north at 7 to 10°. The inner submarine slope marks the location of the Inner Boundary Fault. In the east towards the entrance of the İzmit Bay, the northern and inner submarine slopes converge and form a major westward-sloping canyon (Fig. 3). The 50-km-long Bay of İzmit also has a canyon-type morphology partly overprinted in the centre by the recent deposits of the Hersek delta.

Seismic sections run across the İzmit Bay (Özhan and Bayrak, 1998; Şengör et al., 1999), as well as its canyon-type morphology, indicate that the North Anatolian Fault strikes through the axis of the Bay (Crampin and Evans, 1986; Emre et al., 1999). After its emergence from the Bay, the North Anatolian Fault bifurcates, with the two arms of the fault corresponding bathymetrically to the northern and inner submarine slopes. The bifurcation of the North Anatolian Fault at the western exit of the İzmit Bay can be seen in the seismic line 31 (Fig. 4). In this section, the North and Inner Boundary faults form a steep cusp enclosing a symmetrical basin filled with sediments, up to

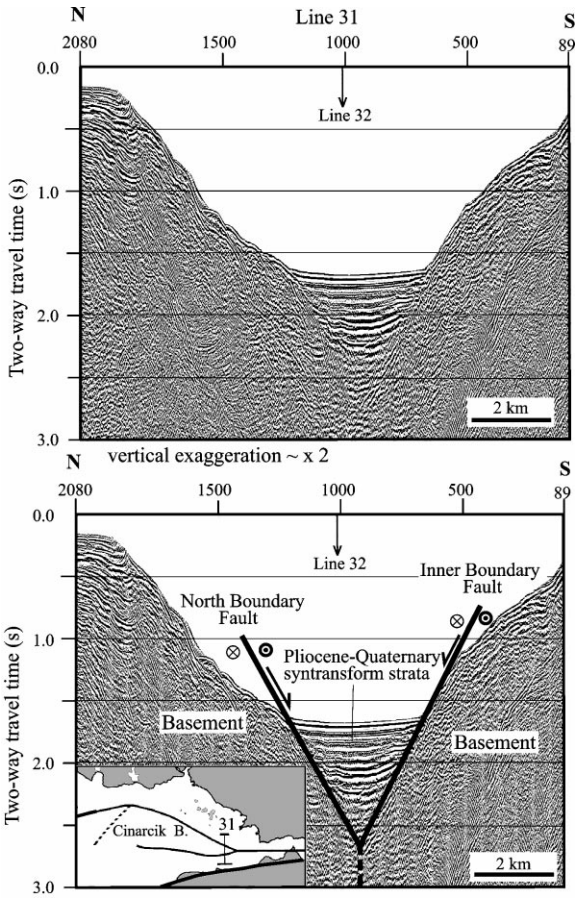

Fig. 4. Uninterpreted and interpreted time-migrated seismic reflection sections of line 31 at the entrance to the İzmit Bay. The digits are the common depth point (CDP) numbers. The vertical exaggeration shown is an average and approximate value for the syntransform sediments. The inset shows the location of the profile in the Çınarcık Basin. See Fig. 3 for a larger-scale profile location.

0.8 s thick (~0.8 km). Both faults merge at about 1 to 1.5 km depth to the subvertical İzmit segment of the North Anatolian Fault forming a symmetrical negative flower structure. As observed in the seismic line 31, the North and Inner Boundary faults follow the contact between the basinal strata and their basement. This can also be recognised in the longitudinal seismic line 32, which runs through the axis of the Çınarcık Basin (Fig. 5). In this section, the base of the basinal strata is a strong reflector, which corresponds to the basal segment of the North and Inner Boundary faults in the seismic line 31 (Fig. 4). This detachment surface dips west and can be followed in the seismic line 32 to a depth of 3.5 km, where it is masked by the multiple reflections (Figs. 5 and 6).

When the North and Inner Boundary faults are traced westwards in the seismic sections, the North Boundary Fault becomes steeper than the Inner Boundary Fault and the resulting negative flower structure attains an asymmetrical geometry (Fig. 6). This can be seen in the seismic line 29, which runs through the centre of the Çınarcık Basin (Fig. 7). In this section, the North Boundary Fault is subvertical, whereas the Inner Boundary Fault dips steeply north enclosing broadly folded young strata. With increasing divergence of the faults towards the west and with increasingly steeper dips, the North and Inner Boundary faults become discrete faults and do not merge to a single fault, at least not in the upper 10 km of the crust. The western part of the Çınarcık Basin has a symmetrical graben-type structure with the North and Inner Boundary faults enclosing a basin filled by flat-lying strata (Figs. 8 and 9a).

The İzmit segment of the North Anatolian Fault has a linear west trend (92°). The trend of the North Boundary Fault north of the Çınarcık Basin is slightly curvilinear, changing from 119° in the east to 107° in the west. The Inner Boundary Fault has a sinuous west trend (94°), subparallel to the İzmit Fault.

The subhorizontal, largely undeformed basinal strata is confined to the Çınarcık depression and hence must have been deposited during the post-Miocene activity of the North Anatolian Fault system. The age of this syntransform sequence is regarded as Pliocene to Quaternary. In the eastern Çınarcık Basin, the syntransform Pliocene–Quaternary strata are truncated at the base by the North and Inner Boundary faults but increase in thickness towards the west and attain a minimum thickness of 2 s, corresponding to ~2 km, in the centre of the basin (Figs. 5 and 8). The basement to the syntransform strata could not be reached in the seismic sections in the western Çınarcık Basin. However, extrapolation from the extreme western part of the seismic line 32, where the syntransform strata are thinnest and dip to the east, indicates that the thickness of the syntransform strata in the

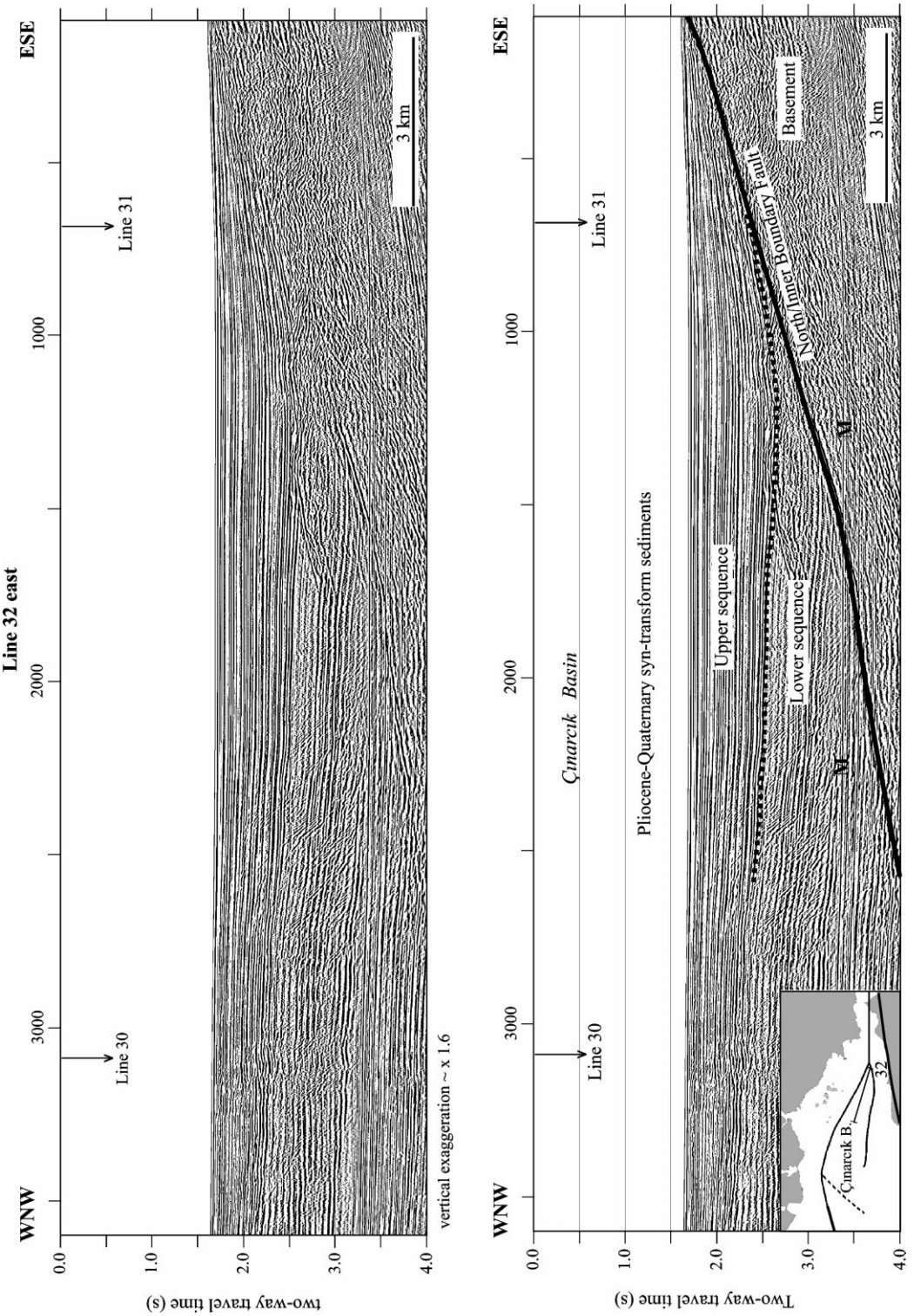

Fig. 5. Uninterpreted and interpreted time-migrated seismic reflection sections of the eastern part of the line 32, which runs along the axis of the Çınarcık Basin. The digits are the common depth point (CDP) numbers. M indicates multiple reflections. The vertical exaggeration shown is an average and approximate value for the syntransform sediments. The inset shows the location of the profile in the Çınarcık Basin. See Fig. 3 for a larger-scale profile location.

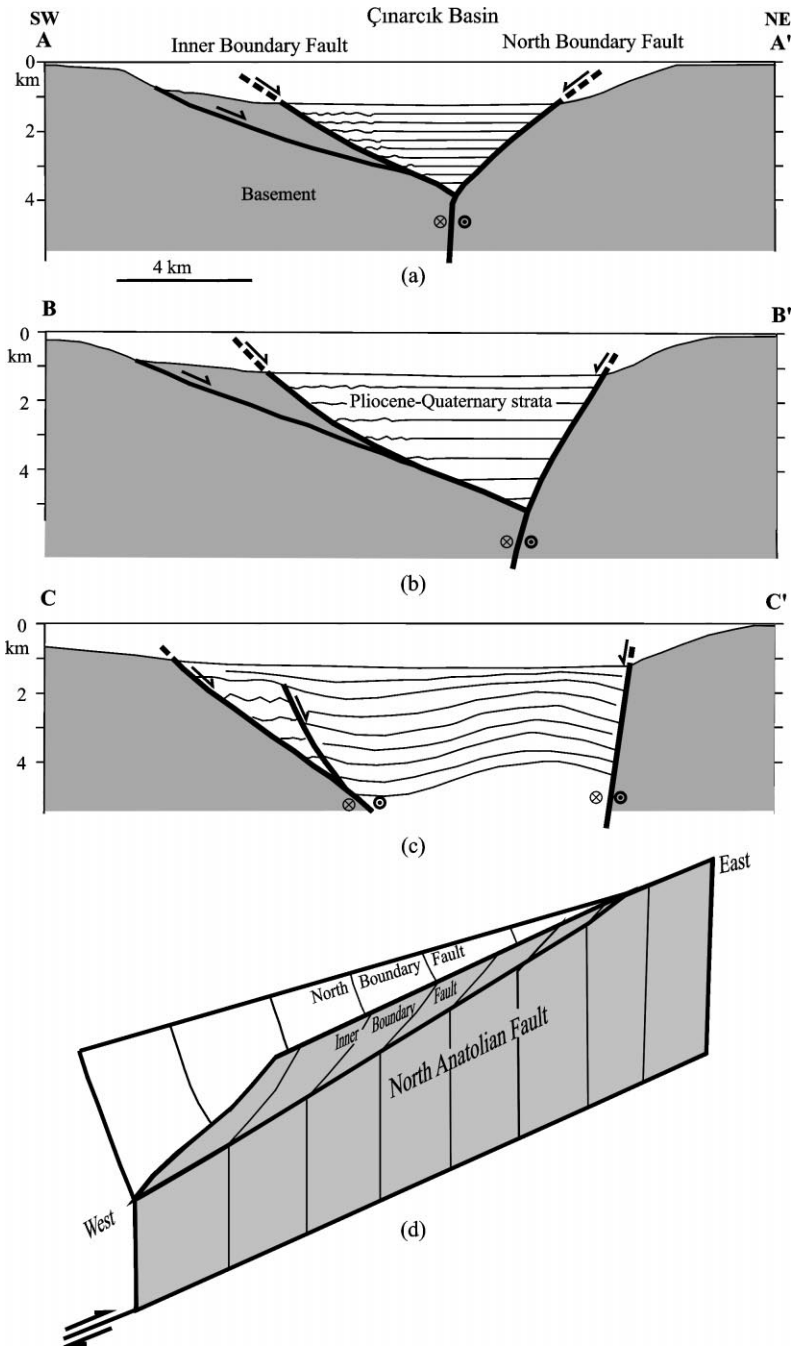

Fig. 6. Unexaggerated cross-sections and a schematic block diagram across the western part of the Çınarcık Basin. For the location of the cross-sections see Fig. 3.

centre of the basin is in excess of 3 km. The syntransform strata dip very gently towards the east ($\sim 3°$) and in the centre of the basin form a gentle anticline–syncline pair with a long wavelength ($\lambda = 11$ km) and possibly with an ENE-trending fold axis (Figs. 6 and 7). Two sequences

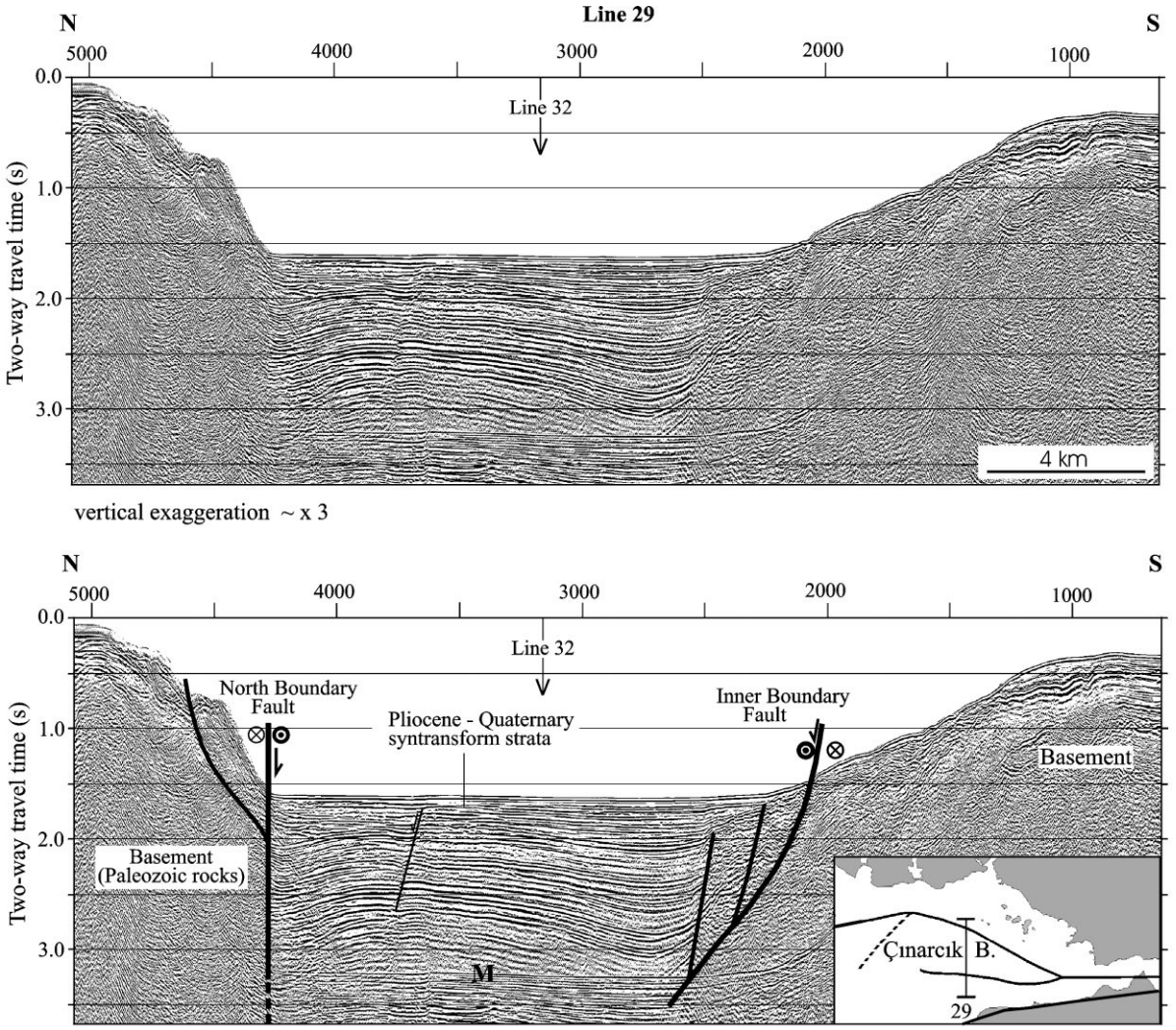

Fig. 7. Uninterpreted and interpreted time-migrated seismic reflection sections of line 29. The digits are the common depth point (CDP) numbers. M indicates multiple reflections. The vertical exaggeration shown is an average and approximate value for the syntransform sediments. The inset shows the location of the profile in the Çınarcık Basin. See Fig. 3 for a larger-scale profile location.

can be distinguished within the syntransform strata in the eastern Çınarcık Basin. The lower of the two sequences becomes thicker towards the east and is truncated by the detachment fault (Fig. 5). The upper sequence also shows a general eastward thickening, but becomes thinner in the vicinity of the detachment fault and rests with apparent conformity on the detachment (Fig. 5). These geometric relations suggest that the upper sequence was deposited within the present fault system, whereas the lower sequence was possibly laid when the North and Inner Boundary faults were not joined at their present depth.

2.3. The Central Marmara Ridge and the Central Ridge Anticlinorium

The Central Marmara Ridge is a northeast-trending submarine high separating the Çınarcık Basin in the east from the Central Marmara Basin

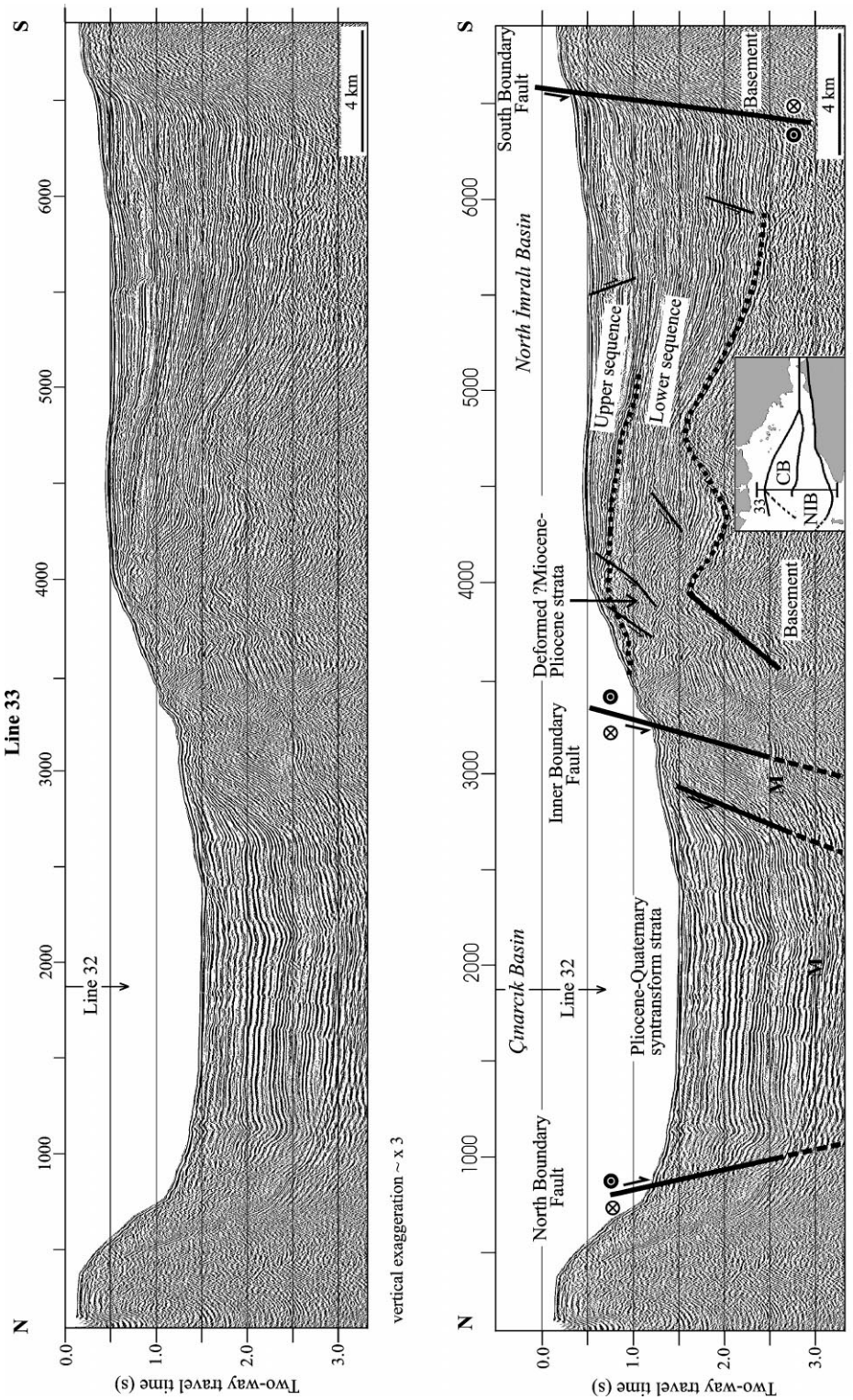

Fig. 8. Uninterpreted and interpreted time-migrated seismic reflection sections of line 33, showing the relation between the Çmarcık and North İmralı Basins. The digits are the common depth point (CDP) numbers. M indicates multiple reflections. The vertical exaggeration shown is an average and approximate value for the syntransform sediments. The inset shows the location of the profile in the Çmarcık (ÇB) and North İmralı (NIB) basins. See Fig. 3 for a larger-scale profile location.

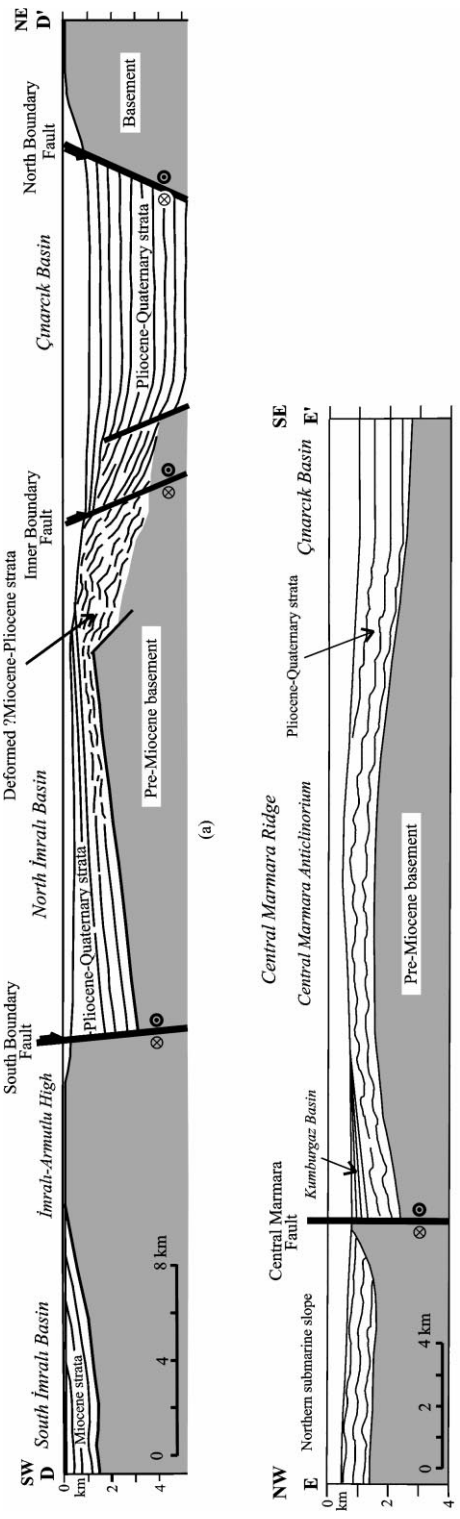

Fig. 9. (a) Unexaggerated cross-section across the Çınarcık, North and South İmralı basins. (b) Unexaggerated cross-section across the Central Marmara Ridge. For the location of the sections see Fig. 3.

in the west (Fig. 2). There is no clear bathymetric boundary between the Çınarcık depression and the Central Marmara Ridge. The Çınarcık depression rises gradually (average slope 3.6° or 6 m/km) to the Central Marmara Ridge with no intervening submarine escarpment. The eastern part of Central Marmara Ridge has a saddle-shaped morphology with the deepest part of the saddle lying about 700 m higher than the adjoining basins (Fig. 3). In its western part there is a small perched depression, named the Kumburgaz Basin, elongated west–southwest. The submarine slope north of the Central Marmara Ridge is wider (up to 12 km) and less steep (4 to 7°) than that north of the Çınarcık depression.

Seismic lines across the Central Marmara Ridge show that the North Boundary Fault makes a restraining bend at 28° 44′, and the resulting segment of the North Anatolian Fault, called the Central Marmara Fault, follows the toe of the northern submarine slope with a strike of ~83° (Fig. 3). It passes through the Central Marmara Basin and joins up with the submarine extension of the Ganos Fault as mapped in the Tekirdağ Basin by Okay et al. (1999) (Fig. 2). The shelf edge north of the Central Marmara Ridge may represent a former continuation of the North Boundary Fault (cf. Fig. 2).

North of the Central Marmara Fault, the wide and shallow northern submarine slope has a Pliocene–Quaternary sedimentary cover, which increases in thickness from zero near the shelf break to ~1.2 km next to the Central Marmara Fault (Figs. 3 and 10). This Pliocene–Quaternary sedimentary cover, not observed on the steep northern submarine slopes of the Çınarcık and Tekirdağ basins (Okay et al., 1999), is partly responsible for the relatively gentle dips of the submarine slope. It has also resulted in slump-related folding in the lower parts of the slope (Figs. 3 and 10).

The Central Marmara Ridge is a northeast-trending broad *anticlinorium*. The anticlinorium has a wavelength of ~22 km and an inter-limb angle of ~162° (9b and Figs. 9b and 11). With increasing inter-limb angle, the anticlinorium fades out southwestward and cannot be recognised in the seismic line M10 (Fig. 3). The anticlinorium is slightly asymmetric, with a shorter and steeper northwestern limb (Figs. 9b and 11). Large numbers of parasitic open folds with half-wavelengths of 0.2–0.7 km occur on both limbs of the Central Ridge anticlinorium (Figs. 11 and 12). The folding, which effects the sea floor morphology, is encroaching on the Çınarcık Basin, as indicated by the small amplitude and small wavelength folds that are nucleating in the sediments of the basin (Figs. 11 and 12). The southeastward-migrating fold-front coincides with the slope break between the Çınarcık basin and the Central Marmara Ridge. The undeformed basinal strata of the Kumburgaz basin, less than 500 m thick, rest on folded sediments of the Central Ridge Anticlinorium (Fig. 11).

Most of the previous studies in the Marmara Sea (e.g. Pfannenstiel, 1944; Barka and Kadinsky-Cade, 1988; Ergün and Özel, 1995; Wong et al., 1995; Barka, 1997) place a northeast-trending dextral strike-slip fault along the Central Marmara Ridge, which would act as a compressive fault segment (cf. Straub and Kahle, 1995). However, seismic sections across the Central Marmara Ridge show that such a fault is not present. Instead the shortening in the Central Marmara Ridge is related to the Central Marmara Fault, which forms a restraining segment with respect to the GPS displacement vectors. The Pliocene–Quaternary sediments of the Çınarcık Basin are translated westwards towards the Central Marmara Fault, which acts as a backstop resulting in the uplift and buckling of the syntransform strata. The Kumburgaz Basin is probably forming under the lee of this large buckle fold. The situation in the Central Marmara Ridge can be compared with the Transverse Ranges in California, where a major bend in the San Andreas Fault causes widespread folding and thrusting (e.g. Crowell, 1979).

2.4. The inner Marmara slope and the Inner Boundary Fault

The inner Marmara slope south of the Çınarcık Basin is about 6 km wide, and is characterised in the seismic profiles by disturbed reflections (7, 8

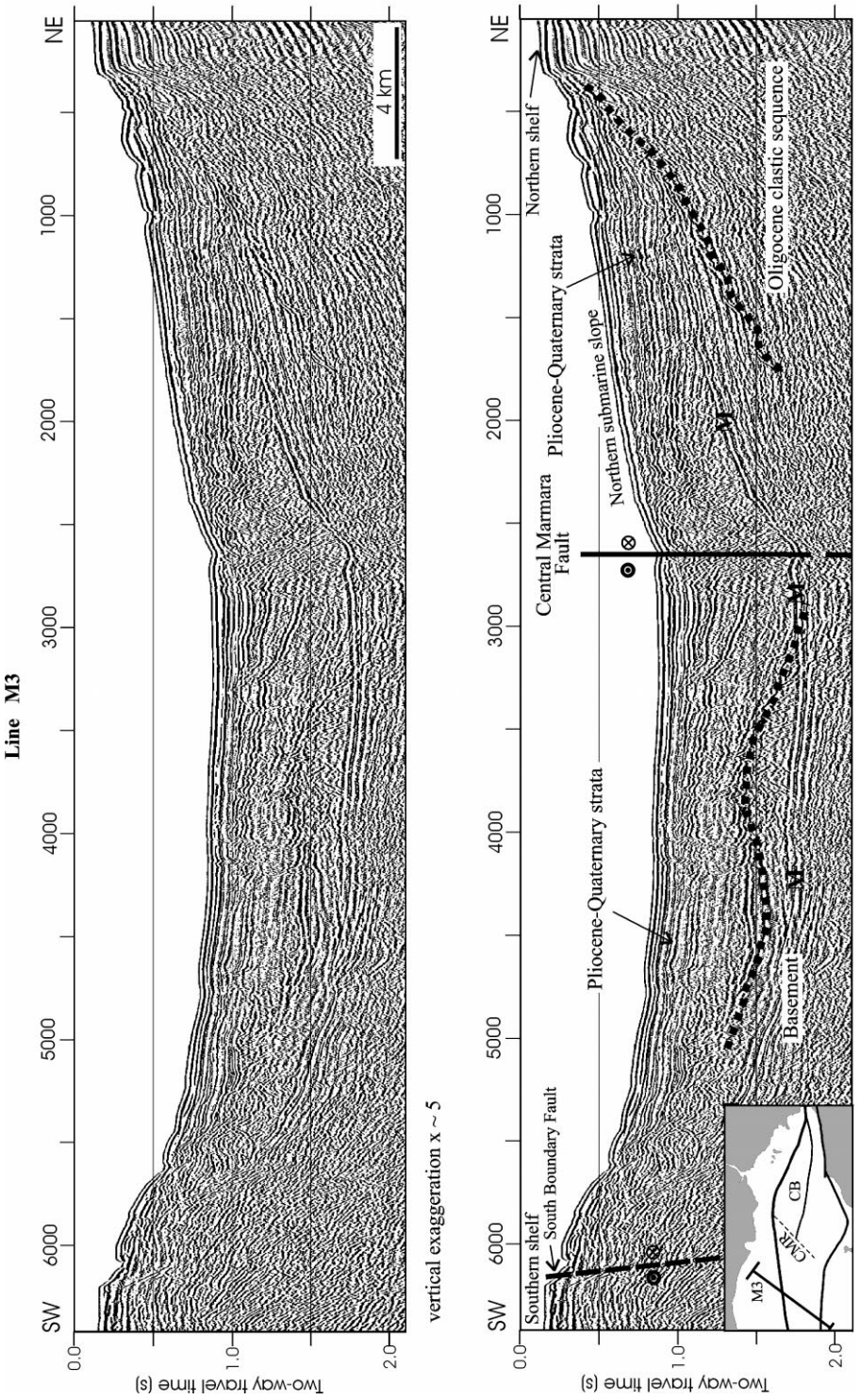

Fig. 10. Uninterpreted and interpreted time-migrated seismic reflection sections of line M3, which runs from the southern to the northern shelf of the Marmara Sea. The digits are the common depth point (CDP) numbers. M indicates multiple reflections. The vertical exaggeration shown is an average and approximate value for the syntransform sediments. The inset shows the location of the profile in the Marmara Sea; CMR: Central Marmara Ridge; CB: Çınarcık basin. See Fig. 3 for a larger-scale profile location.

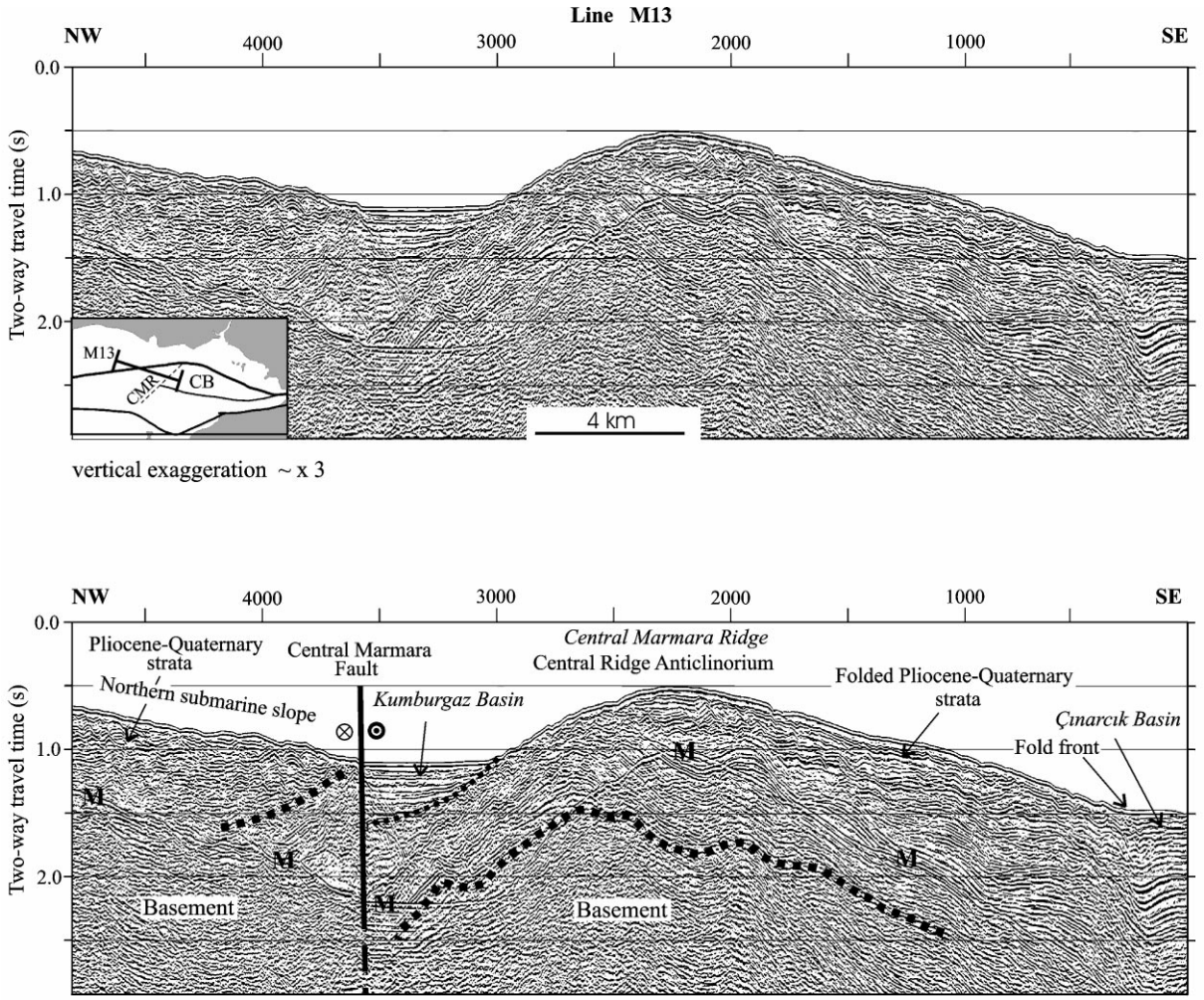

Fig. 11. Uninterpreted and interpreted time-migrated seismic reflection sections of line M13, which runs across the Central Marmara Ridge. The digits are the common depth point (CDP) numbers. M indicates multiple reflections. The vertical exaggeration shown is an average and approximate value for the syntransform sediments. The inset shows the location of the profile in the Marmara Sea; CMR: Central Marmara Ridge; CB: Çınarcık Basin. See Fig. 3 for a larger-scale profile location.

and Figs. 7, 8 and 13). In the seismic section 37, these scattered reflections are seen to lie over the basement (Fig. 13) suggesting that the upper levels of the inner Marmara slope consist of deformed Miocene and younger strata. The deformation is characterised by disharmonious, rootless folds, probably of slump origin, which do not affect the pre-Miocene basement. The main strand of the Inner Boundary Fault appears to be located near the basin-slope break. One splay of the Inner Boundary Fault cuts the Pliocene–Quaternary syntransform sediments in the basin but is also overlain by as yet undeformed Pliocene–Quaternary strata, ~100 m thick (Figs. 7 and 9a). The wedge of Pliocene–Quaternary strata between this splay and the main strand of the Inner Boundary Fault is deformed. The inner submarine slope, when traced eastward, is seen to be associated with a low-lying strip of Upper Miocene–Pliocene sediments in the Armutlu Peninsula (Fig. 3). This Neogene sequence is probably representative of the rocks of the inner Marmara slope.

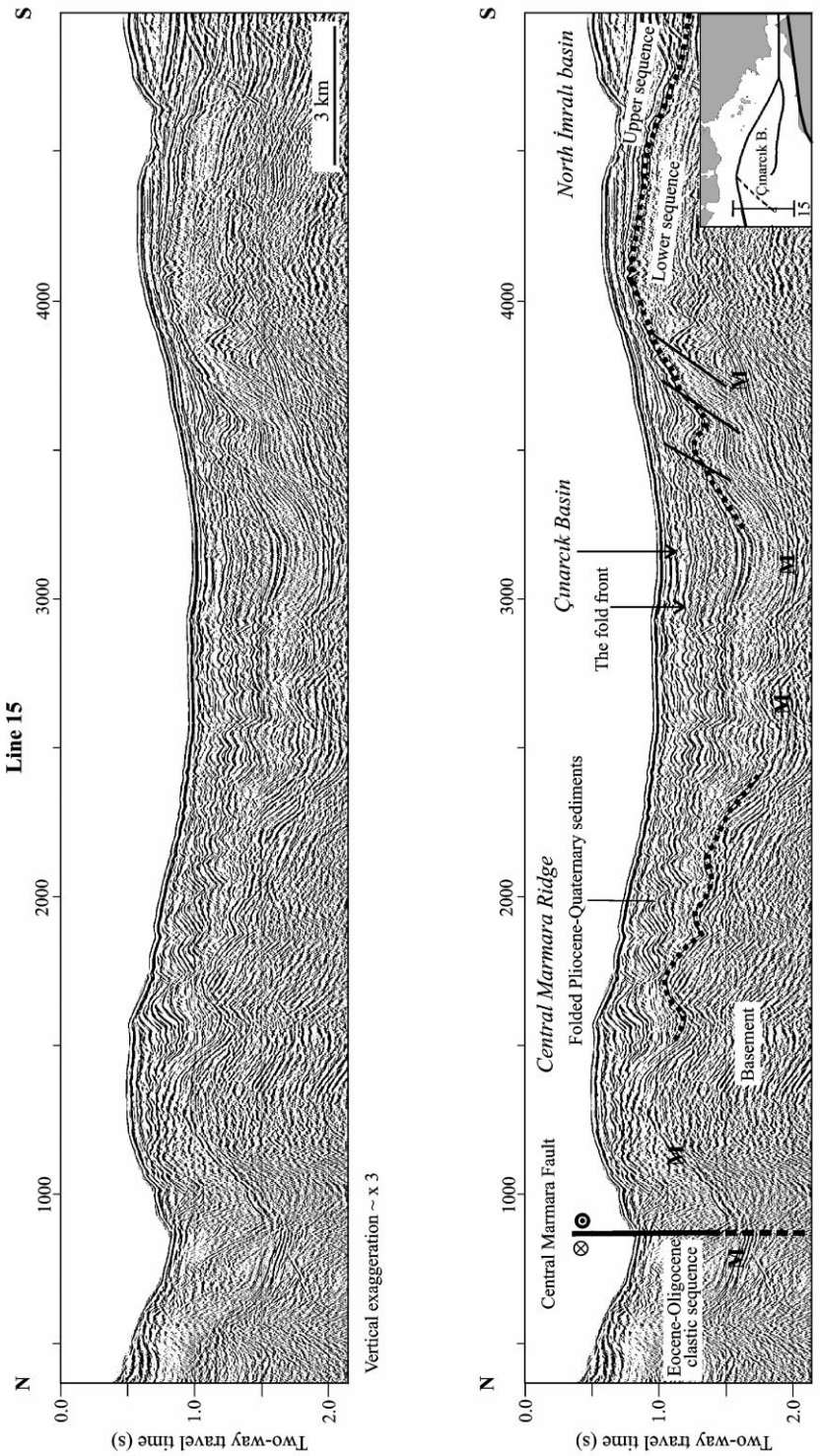

Fig. 12. Uninterpreted and interpreted time-migrated seismic reflection sections of line 15, which runs along the Central Marmara Ridge. The digits are the common depth point (CDP) numbers. M indicates multiple reflections. The vertical exaggeration shown is an average and approximate value for the syntransform sediments. The inset shows the location of the profile in the eastern Marmara Sea. Fig. 3 for a larger-scale profile location.

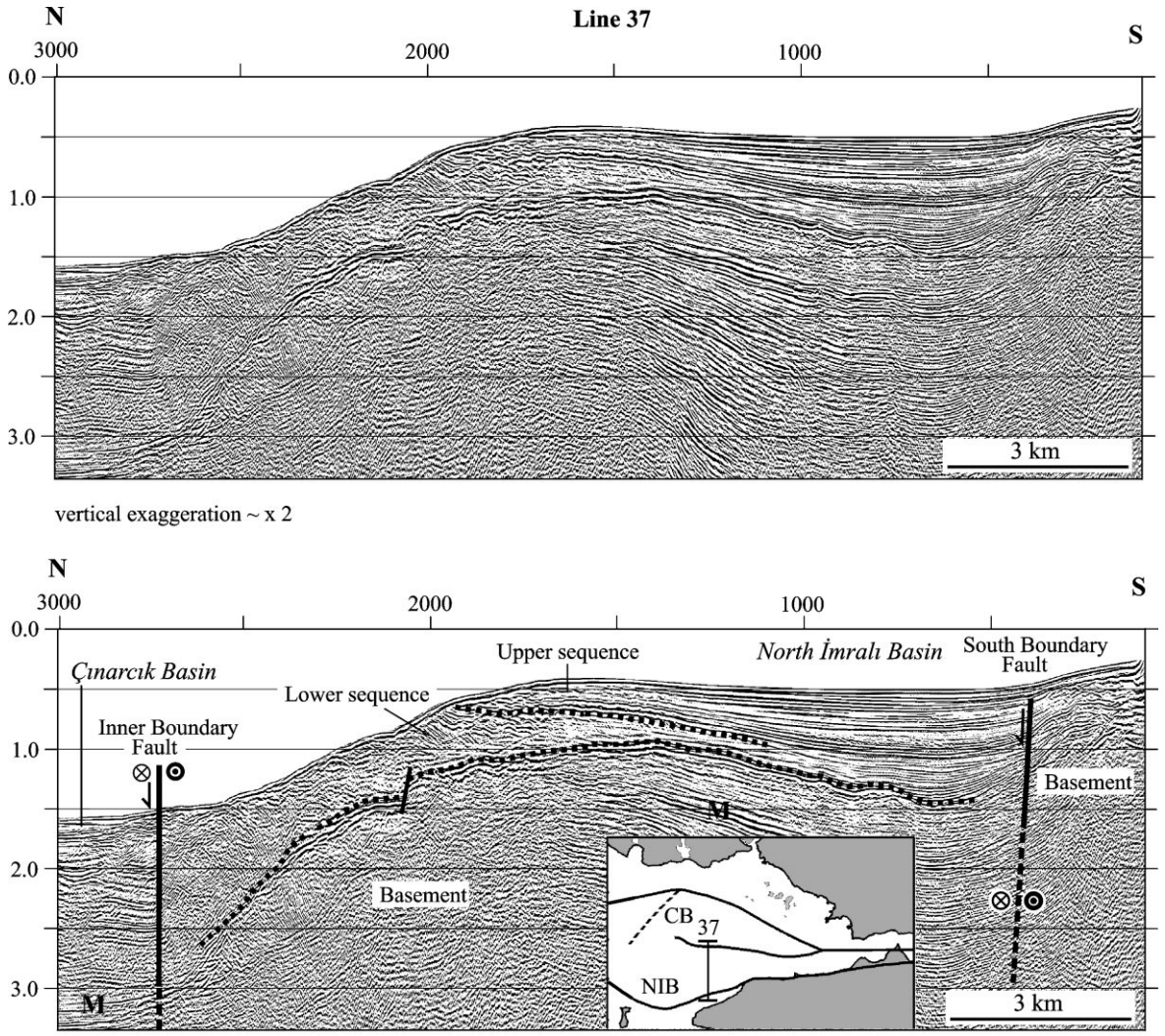

Fig. 13. Uninterpreted and interpreted time-migrated seismic reflection sections of line 37. The digits are the common depth point (CDP) numbers. The vertical exaggeration shown is an average and approximate value for the syntransform sediments. The inset shows the location of the profile in the eastern Marmara Sea. See Fig. 3 for a larger-scale profile location.

2.5. Neogene sediments on the Armutlu Peninsula

The southern margin of the Marmara Sea, including the Armutlu Peninsula, has a complex geology with a wide variety of Palaeozoic to Eocene metamorphic, magmatic and sedimentary rocks (Yılmaz et al., 1995; Okay et al., 1996). Hercynian (Carboniferous), Cimmeride (Late Triassic) and Alpide (Palaeocene–Early Eocene) orogenies have affected the region. Miocene and younger terrigenous sedimentary rocks rest unconformably on this complex basement. The lower parts of the Neogene sequence consist of Upper Miocene marl and mudstone with rare sandstone and gypsum intercalations, about 700 m thick (Akartuna, 1968). This is overlain unconformably by another sequence of marl, mudstone, limestone, sandstone, conglomerate and lignite of Upper Miocene (Pontian) to Pliocene age. Lacustrine limestones within this sequence form lenses up to

100 m thick. Some of these carbonate lenses contain vertebrate fossils dated as the middle part of the Early Pliocene (Akartuna, 1968).

2.6. The South Boundary Fault and the deep shelf — the site of the North İmralı Basin

The deep shelf is a broad submarine depression with an average depth of −400 m between the Çınarcık Basin in the north and the southern shelf in the south (Fig. 3). It is bounded in the north by a west-trending subdued submarine ridge, which rises about 50 m above the floor of the deep shelf (Fig. 3). In the south, the deep shelf is separated via the narrow southern submarine slope from the broad southern shelf. The southern submarine slope corresponds to a major fault, named the South Boundary Fault by Wong et al. (1995). The deep shelf pinches out towards the east, whereas in the west it extends without a break towards the Central Marmara Ridge.

Seismic sections show that, in the eastern Marmara Sea, the South Boundary Fault consists of northeast- (70–80°), northwest- (107–122°) and west-trending (90°) submarine segments. The deep shelf, bounded by the northwest- and northeast-trending fault segments, corresponds to an asymmetrical basin, named here as the North İmralı Basin (Fig. 3). The strata in the basin thicken and dip gently (up to 6°) towards the northwest-trending fault segment (Figs. 8, 12 and 13). The basinal sediments next to the northwest-trending fault segment have a thickness in excess of 2.5 km, indicating major vertical displacements along this segment. This observation and the azimuth of the regional displacement vector indicate that the North İmralı basin is a fault-bend strike-slip basin, forming in front of the northwest-trending releasing fault bend. In terms of geometry and basin fill, it is similar to the Tekirdağ Basin in the eastern Marmara Sea (Okay et al., 1999). Such asymmetric strike-slip basins indicate extension at right angles to the strike-slip fault and imply simultaneous strike-slip motion and transform normal extension (Aydın et al., 1990; Ben-Avraham and Zoback, 1992). The bathymetrically deepest part of the deep shelf corresponds to the region with the maximum sedimentary thickness (Fig. 3), suggesting on-going development of the North İmralı Basin. In contrast to the active nature of the faults bounding the North İmralı Basin, the western extension of the South Boundary Fault is poorly defined on the seismic section M3 (Fig. 10).

In the seismic sections, the northeast-trending fault segment bounding the North İmralı Basin can be traced eastwards to a previously known active fault marking the rectilinear northern coast of the Armutlu Peninsula (Akartuna, 1968; Şaroğlu et al., 1992). This Armutlu Fault trends along the northern margin of the Armutlu Peninsula for 65 km before joining the İzmit segment of the North Anatolian Fault in the eastern part of the İzmit Bay (Fig. 2).

The infill of the North İmralı Basin consists of two sedimentary sequences differentiated mainly by their degree of deformation. In the northern part of the basin, the lower sedimentary sequence is deformed with rootless folds and shallowly northward-dipping normal faults (Figs. 8 and 13). The lower sedimentary sequence can be observed on the seismic line 33 to continue into the southern slope (Figs. 8 and 9), suggesting that it probably consists of Upper Miocene–Lower Pliocene marl and mudstone exposed on land in the Armutlu Peninsula. The much less deformed upper sequence, which onlaps the top part of the southern slope, lies unconformably over the lower sequence (Figs. 8 and 12). However, the deformation in the lower sedimentary sequence decreases towards the south and the separation of the lower and upper sequences becomes difficult in the central part of the North İmralı Basin (Figs. 8, 9 and 13), indicating that the deformation is related to the Inner Boundary Fault Zone.

2.7. Facies of the basinal sediments in the eastern Marmara Sea

There is only one offshore well in the Marmara Sea, which constrains the facies of the basinal sediments in the Çınarcık and North İmralı basins. The Marmara-1 (M-1) well, drilled at the western limit of the North İmralı basin (Fig. 3), has cut through less than 40 m of Quaternary marine clays

overlying Upper Miocene(?)–Pliocene terrigeneous sediments, 2100 m in thickness (Marathon Oil Company, 1975; Ergün and Özel, 1995). The terrigeneous sequence can be subdivided into two formations. The upper formation consists of Lower Pliocene brackish to fresh water marl, ~80 m thick, whereas the lower unit is made up of Upper Miocene(?)–Pliocene sandstone and mudstone with minor limestone, tuff and lignite, 2022 m thick, deposited in a fluvio-deltaic environment. This sequence rests unconformably over pelagic Cretaceous limestones, which outcrop on the Island of İmralı (Erguvanlı, 1949). The Upper Miocene–Pliocene sequence in the Marmara-1 well is similar in facies to that described from the Armutlu Peninsula (Akartuna, 1968; Bargu and Sakinç, 1993). Thus, the onshore and offshore stratigraphic data indicate that the Marmara Sea was a land area during the Pliocene. The first fully marine conditions in the Marmara Sea are recorded in the Pleistocene marine terraces south of the İzmit Bay, which lie up to 70 m above sea level (Fig. 3, Erinç, 1955; Sakinç and Bargu, 1989). The shells in the terraces have been dated by U/Th method as Mid- to Late-Pleistocene (260 000–130 000 years, Paluska et al., 1989). Fauna in these terraces is typically Mediterranean, indicating influx from the Aegean Sea.

The arguments cited above suggest that the basinal sediments in the Çınarcık and North İmralı basins are predominantly terrigeneous clastics. The considerable thickness of syntransform strata in a relatively small area suggests that during the Pliocene both the Çınarcık and North İmralı depressions were probably occupied by lakes.

2.8. *The southern shelf and the South İmralı Basin*

The southern shelf is a 20-km-wide flat-lying region at a water depth of less than 110 m. İmralı Island and the Gemlik Bay are located within the southern shelf (Fig. 3). The northern part of the shelf between the İmralı Island and the Armutlu Peninsula is seen in the seismic sections to be a high standing area with little or no basinal sediments (Figs. 9 and 14). This Armutlu–İmralı high represents the footwall block of the Armutlu Fault, and has been undergoing footwall uplift during the vertical displacements along the Armutlu Fault. It must have been a land area during the latter part of the Quaternary, where the sea level has been close to −50 m (Chappell and Shackleton, 1986). The western part of the Armutlu Peninsula is made up of metamorphic rocks, granites and Eocene volcanic rocks (Akartuna, 1968), whereas the northern part of the İmralı Island consists of Upper Cretaceous limestones (Erguvanlı, 1949). Similar basement rocks are expected in the Armutlu–İmralı high and farther west in the southern shelf. In the seismic sections, there is a belt of unreflective basement south of the İmralı Fault, which might represent a buried sheet-like igneous intrusion (Fig. 14). A south-dipping (~5°) and southward-thickening sedimentary sequence drapes over this basement in the south (Fig. 14). Isopachs of sedimentary thickness in seconds two-way travel time of this South İmralı Basin are shown in Fig. 3. At the southern limit of the seismic lines, the basinal strata reach a thickness of 1 s, corresponding to about 1 km. Southward extrapolation from the seismic sections suggests that the basinal sediments increase in thickness to about 1.5 km near the coast. As Eocene and older rocks are exposed in the immediate onshore (Fig. 2), the sediments of the South İmralı Basin must be truncated by a major offshore fault trending close and parallel to the coastline. Further evidence for the presence of this coastal fault is provided by the geomorphology of the coastline between Tirilye and Bandirma. This coastline is straight with a steep coastal slope, and the drainage divide lies very close to the sea (Fig. 3). This coastal fault is part of a series of east-trending fault segments that extend eastward to the Lake of İznik (Fig. 3).

The sediments of the South İmralı Basin are partly exposed on land in the southern part of the İmralı Island (Fig. 3). They form a gently southward-dipping sequence, lying unconformably over the Upper Cretaceous limestones (Erguvanlı, 1949). The sediments are made up of terrigeneous mudstone, marl, conglomerate, sandstone with a minimum thickness of 250 m. The sedimentary beds strike north-northwest and dip at 10–12° to

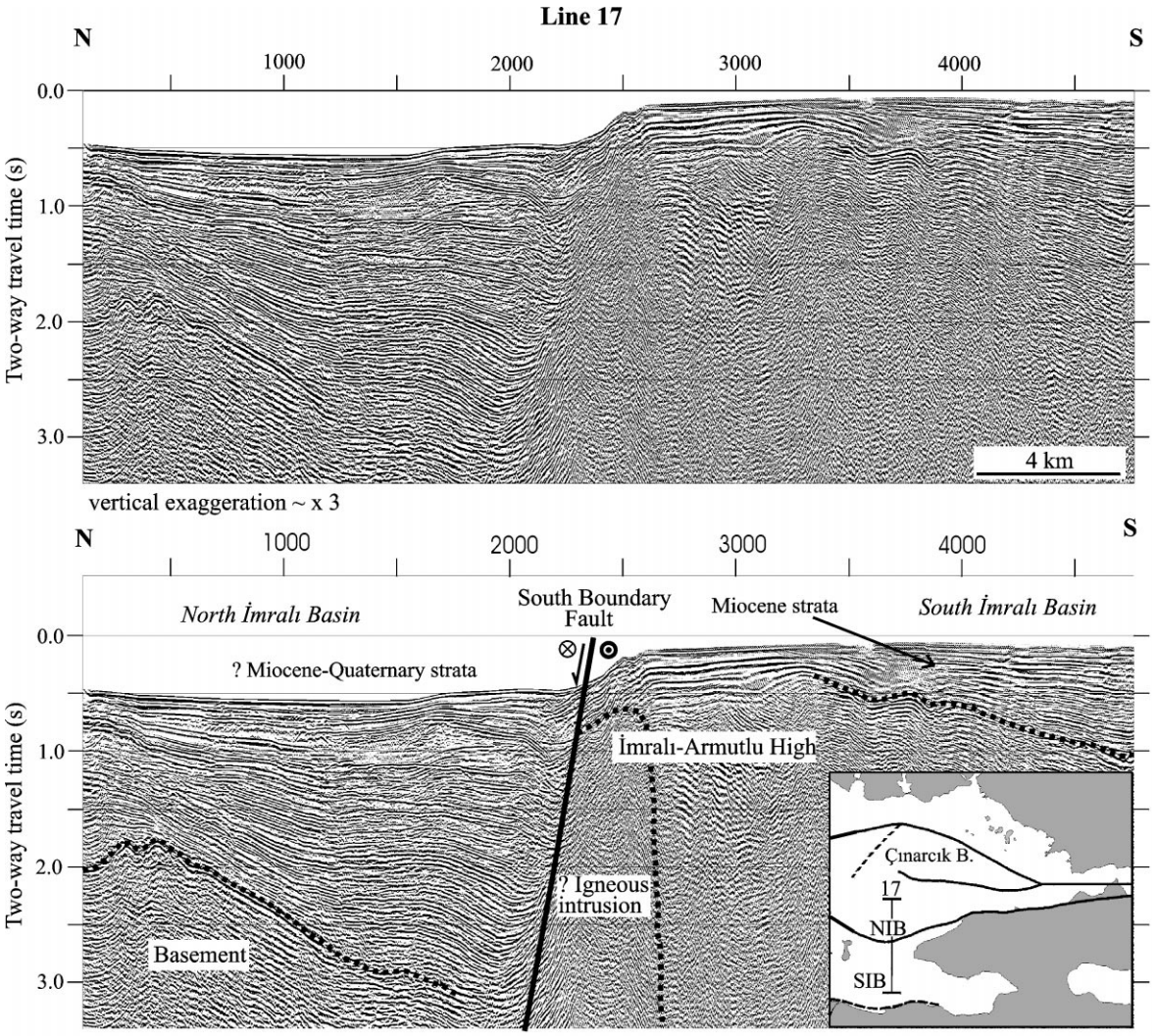

Fig. 14. Uninterpreted and interpreted time-migrated seismic reflection section of line 17. The digits are the common depth point (CDP) numbers. M indicates multiple reflections. The vertical exaggeration shown is an average and approximate value for the syntransform sediments. The inset shows the location of the profile in the eastern Marmara Sea. See Fig. 3 for a larger-scale profile location.

the southwest similar to that observed in the seismic sections in the South İmralı Basin. Although no fossils have been found in these terrigeneous sediments, a Neogene age (possibly Miocene) is assigned to the sequence based on correlation with similar sequences on land (Erguvanlı, 1949).

The subareal exposure of the sediments of the South İmralı Basin (Fig. 3) indicates that the strata of the South İmralı Basin have been uplifted and partly exhumed since their deposition. In this aspect the South İmralı Basin is different from the evolving Çınarcık and the North İmralı basins, where there may have been continuous deposition at least since the early Pliocene. The lack of correlation between the bathymetry and the sedi-

mentary thickness in the South İmralı Basin also indicates that, unlike the Çınarcık and North İmralı basins, the South İmralı Basin is inactive.

3. Origin of the Çınarcık Basin

The Çınarcık depression has been generally interpreted as a pull-apart basin (Şengör et al., 1985; Barka and Kadinsky-Cade, 1988; Wong et al., 1995). Pull-apart basins are rhomb-shaped depressions bounded on their sides by two subparallel, overlapping strike-slip faults, and at their ends by perpendicular or diagonal dip-slip faults (e.g. Crowell, 1974; Aydın and Nur, 1982; Mann et al., 1983; Sylvester, 1988; Ingersoll and Busby, 1995). In contrast to these features, the Çınarcık Basin is wedge-shaped and is bounded by two diverging fault splays. Therefore, it would be more appropriate to label the Çınarcık Basin as a releasing fault-wedge basin (Crowell, 1974) forming at a junction of the North Anatolian Fault. Fig. 15 shows schematically the present mode of opening of the Çınarcık Basin. At the fault junction, the North Boundary Fault forms a releasing bend, and the Çınarcık Basin is being translated westwards along the North and Inner Boundary faults, similar to that envisaged for the Ridge Basin in California by May et al. (1993). The restraining Central Marmara Fault causes shortening, folding and uplift of the sediments of the Çınarcık Basin in the west. Although this model explains the present opening of the Çınarcık Basin, it does not explain its wedge-shape and the origin of the major restraining bend between the North Boundary and Central Marmara faults. Here, we propose a model that provides an explanation for these features, as well as for the origin of the NW- and SW-trending dextral strike-slip faults in the Thrace and in the Biga Peninsula (Fig. 2).

The initial formation of the Çınarcık Basin can be modelled using the evolution of a dextral transform–transform–transform (TTT)-type triple junction (Fig. 16). The arms of the triple junction correspond to the İzmit segment of the North Anatolian Fault in the İzmit Bay, the North Boundary Fault and the Biga Fault in the Biga Peninsula (Fig. 2). The Inner Boundary Fault,

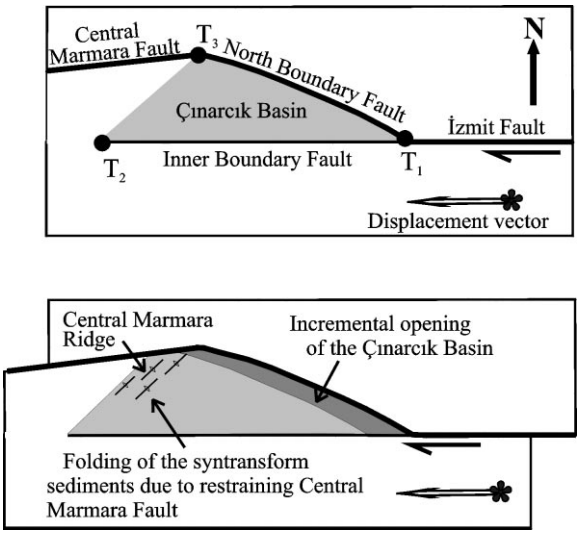

Fig. 15. Schematic plan view illustrating the present mode of opening of the Çınarcık Basin at a releasing fault junction of the North Anatolian Fault. The restraining Central Marmara Fault causes folding and uplift of the syntransform sediments resulting in the Central Marmara Ridge. Simultaneous extension and shortening occur in area of less than 40 km across. The extension is shown to happen along the northeastern rim of the basin; in reality it is distributed throughout the basin. The solid circles T_1 to T_3 represent tie-points; the distance between T_1 and T_2 gives the displacement along the main North Anatolian Fault during the triple junction phase of the Çınarcık Basin. See text and Fig. 16 for further details.

which is subparallel to the İzmit Fault, is considered as part of the İzmit Fault. The North Boundary and the Biga faults make angles of 153° and 37° respectively with the İzmit Fault (Fig. 2). These three faults define three blocks named the Eurasian, Anatolian and Marmara blocks. Dextral strike-slip movement along these North Anatolian faults of the TTT-triple junction creates a wedge-shaped basin similar in outline to the Çınarcık Basin (Fig. 16b and c).

The TTT-triple junction model predicts that the Çınarcık Basin started to develop in the east and progressed westward with the gradual increase in the width of the basin. The westward decrease in the thickness of basinal sediments in the Çınarcık Basin, as observed in the seismic sections, is in accordance with this prediction. A further and more stringent prediction of the TTT-triple junction model is that the North Boundary Fault

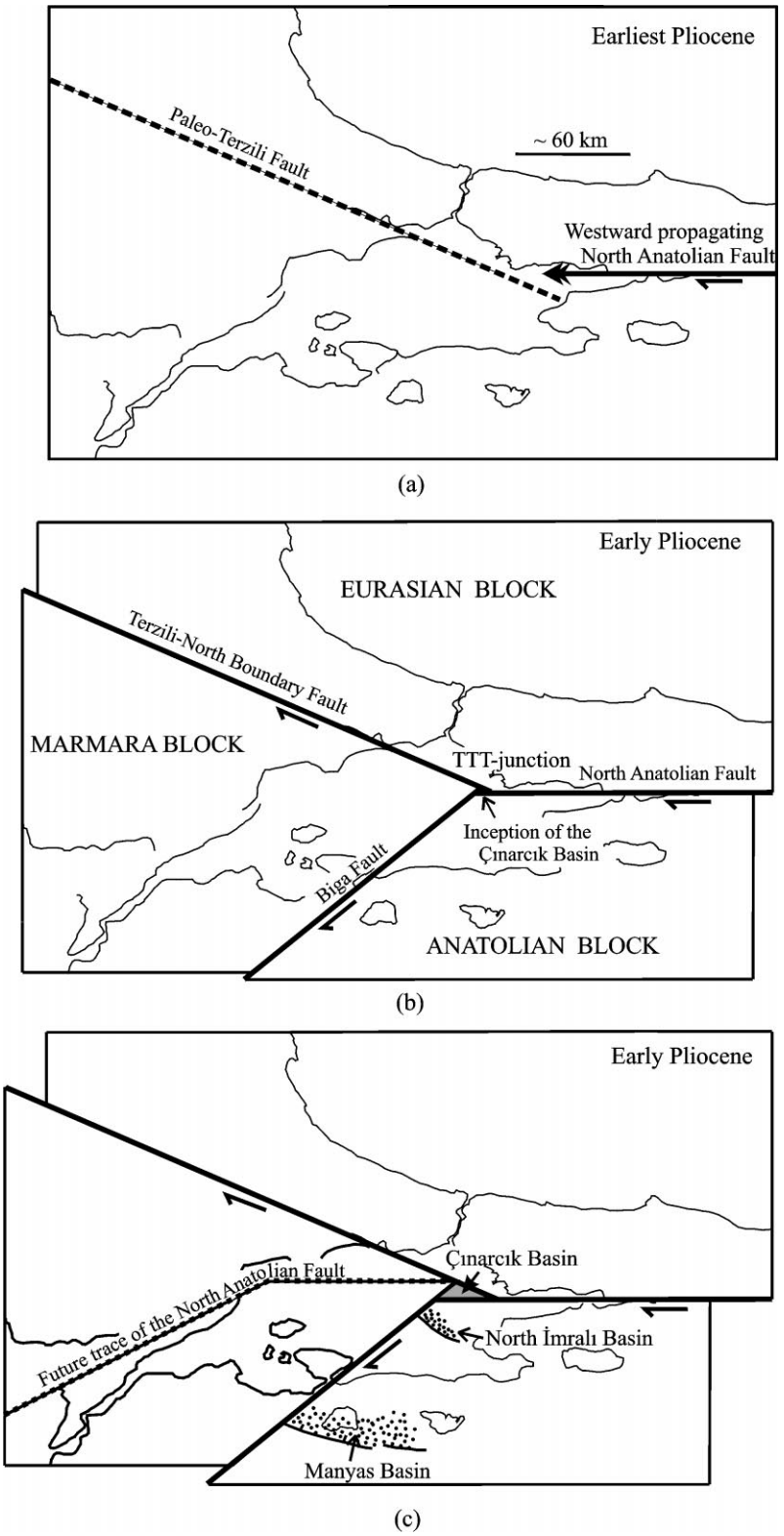

Fig. 16. Tectonic model for the early evolution of the North Anatolian Fault in the Marmara region. See text for further details.

should extend along strike much farther than its present length.

3.1. Former extension of the North Boundary Fault into the Thrace

Most of the southern and central Thrace consists of an Eocene–Lower Miocene clastic basin with over 8-km-thick sediments in its central part (e.g. Turgut et al., 1991; Görür and Okay, 1996). Because of its gas and petroleum potential, a dense network of seismic lines and large number of boreholes are available in the Thrace Basin. Based on the interpretation of these seismic lines, Perinçek (1991) and Turgut et al. (1991) described in the central Thrace a northwest-trending, inactive dextral strike-slip fault zone of over 140 km in length (Fig. 2). This Terzili Fault zone is traced in the Eocene–Lower Miocene sedimentary rocks from around the Marmara Sea to Edirne near the Turkish–Bulgarian border, but is not reported from the crystalline rocks of the Rhodope Massif across the border (Fig. 2). The Terzili Fault zone is marked in the seismic sections by flower structures, releasing and restraining bends, and en echelon folds in the Eocene–Lower Miocene sediments; the latter are hosts to several commercial gas fields (Perinçek, 1991; Turgut et al., 1991). These structures indicate a dextral strike-slip movement along the Terzili Fault.

Along most of its length, the Terzili Fault zone is concealed beneath a layer of fluviatile clastic sediments, up to 1000 m thick (Perinçek, 1991; Turgut et al., 1991). There is also no current or historical seismicity associated with the Terzili Fault (Üçer et al., 1985; Crampin and Evans, 1986; Jackson, 1994). The Terzili Fault crops out underneath this cover in the northern margin of the Marmara Sea (Fig. 2). The sparse outcrop in this coastal plain does not allow mapping of the Terzili Fault. However, the fault zone can be observed in the seismic sections west of Silivri. A Turkish Petroleum Company (TPAO) seismic section across the Terzili Fault close to the Marmara Sea is shown in Fig. 17. In this section the Terzili Fault forms a positive flower structure in the Upper Oligocene sandstones. The Terzili Fault must extend in the shelf area towards the North Boundary Fault; however, the seismic sections in the shelf area are not informative because of strong multiples.

The upper age of the Terzili Fault is constrained by the poorly cemented boulders, sands and clays, which unconformably overlie the fault zone. These fluviatile sediments are regarded either as Pliocene (Keskin, 1974; Perinçek, 1991; Turgut et al., 1991) or Pliocene–Pleistocene in age (Kopp et al., 1969). The presence of the vertebrate fossil *Hipparion* sp. in the clastics rocks (Umut, 1988) indicates that they cannot be older than Pliocene (Sickenberg and Tobien, 1971). Thus, the activity along the Terzili Fault can be constrained between the Mid-Miocene and Pliocene. Turgut et al. (1991) and Perinçek (1991) regarded the Terzili Fault as an early splay of the North Anatolian Fault, but the kinematic relation to the west-trending main North Anatolian Fault remained unclear. It is suggested here that the Terzili Fault, which lies along strike of the North Boundary Fault, constituted its northwestward extension during the TTT-triple junction phase of the Çınarcık Basin (Fig. 16b). The termination of the TTT-triple junction opening and the onset of the present-day fault geometry in the Marmara Sea must have occurred in the Pliocene, as shown by the age of the unconformable cover over the Terzili Fault.

3.2. Biga Fault in the Biga Peninsula

A postulate of the TTT-triple junction model is that a major inactive fault, originating at the fault bend between the North Boundary and Central Marmara faults, should extend southwestward under the Central Marmara Ridge and southern shelf into the northwest Anatolia. The presence of this inactive dextral strike-slip fault under the southern shelf cannot be tested because of the absence of seismic sections in the shelf. However, a southwest-trending dextral strike-slip fault zone is known from the Biga Peninsula (Barka and Kadinsky-Cade, 1988), which may constitute the extension of the postulated strike-slip fault. This Biga Fault zone cuts the Triassic and older sedimentary and metamorphic rocks as well as the Miocene continental sediments and extends from the Kapıdağ Peninsula to the Gulf of Edremit for

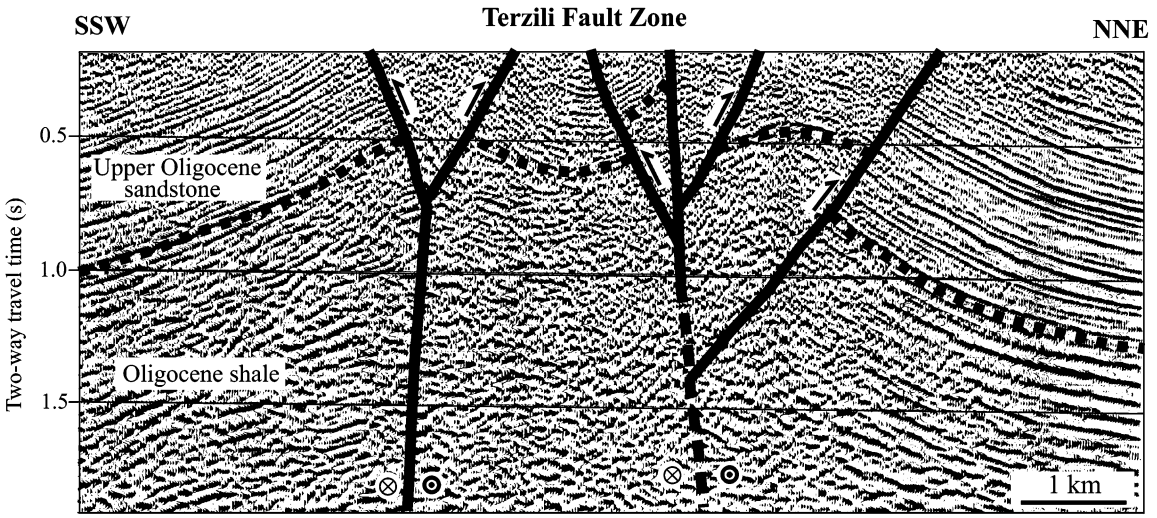

Fig. 17. Interpreted time-migrated TPAO seismic reflection section, which runs across the Terzili Fault close to the Marmara Sea. See Fig. 2 for the profile location.

a distance of over 90 km (Fig. 2). The displacement of the pre-Tertiary strata along one fault strand within the Biga Fault zone indicates a dextral offset of 8 km (Siyako et al., 1989). The trend of the Biga Fault Zone is subparallel to the present-day slip vectors (cf. Fig. 2). Therefore, unlike the Terzili Fault, the Biga Fault zone is active. A fault segment between Yenice and Gönen, ~50 km long, was reactivated during a major earthquake (M_S 7.2) in 18.3.1953 with up to 4 m of dextral displacement (Ketin and Roesli, 1953). The Biga Fault zone most probably connects through the southern shelf of the Marmara Sea to the segment boundary between the North Boundary and Central Marmara faults, which lies along its projected trend (Fig. 2).

4. Origin of the North İmralı Basin

The North İmralı Basin is bounded by the NW-trending transtensional segment of the Armutlu Fault. A similar WNW-trending transtensional fault limits the on-land Manyas Basin in the south (Fig. 2). These NW- to WNW-trending transtensional faults, bounding the North İmralı and Manyas basins, terminate against the Biga Fault zone, implying kinematic coupling between the dextral strike slip movement and normal faulting. The North İmralı Basin, as well as the similarly oriented Manyas Basin in the south (Fig. 2), were probably initiated, or their subsidence accelerated, as a result of the internal distension of the western margin of the Anatolian block during the TTT-triple junction phase (Fig. 16c).

The TTT-triple junction model is strictly applicable to the oceanic lithosphere (McKenzie and Morgan, 1969). The deformation in the continental lithosphere is known to be generally more diffuse and not solely concentrated on plate boundaries. However, of the three blocks around the TTT-triple junction, the Eurasian and the Marmara blocks have behaved rigidly during the period of the opening of the Çınarcık Basin, whereas the western margin of the Anatolian block was dissected by NW- to WNW-trending normal faults. These faults must have accommodated some of the southwestward translation of the Anatolian block. The north–south extension in the Aegean is known to have been active, at least, since the Mid-Miocene, ~11 Ma (Le Pichon and Angelier, 1979). Therefore, in the Pliocene (~5 Ma), when the North Anatolian Fault propagated into the Marmara region, the western margin of the Anatolian block was already dissected by west-trending normal faults, and hence was more condu-

sive to internal deformation than the relatively undeformed Eurasian and Marmara blocks.

5. Propagation history of the North Anatolian Fault

5.1. Total displacement of the North Anatolian Fault in the Marmara region

The TTT-triple junction model provides a piercing point, in terms of the unstable triple junction itself, to estimate the offset along the North Anatolian Fault system in the Marmara region. The point of origin of the triple junction in the western exit of the İzmit Bay, as well as its present location along the Central Marmara Ridge, are fairly tightly constrained, and indicate a total displacement of 52 km during the TTT-triple junction phase (Figs. 3 and 15). The post-TTT displacement is more difficult to quantify, but is at least equal to the ~ 1 km shortening across the Central Marmara Ridge. Further dextral displacements must have occurred along the Inner Boundary and South Boundary faults, and along the fault zone south of the İznik Lake (Fig. 2). The Inner Boundary Fault appears to die out westward (Fig. 2), suggesting a minor total offset (<5 km?). The fault zone south of the İznik Lake, generally regarded as a major branch of the North Anatolian Fault (e.g. Şengör, 1979; Barka, 1997), consists of short fault segments, 10 to 20 km long, with major vertical displacements (Fig. 2). These are typical features of normal fault zones (e.g. Paton, 1992). Furthermore, the seismic sections indicate that the İznik Fault zone does not continue as a major fault into the Gemlik Bay (Fig. 3). Therefore, the dextral offset along the İznik Fault zone is most probably minor (<1 km). The offset along the South Boundary Fault is more difficult to quantify, but is probably much less than that along the North Boundary and Central Marmara faults.

The minimum total offset along the North Anatolian Fault system in the eastern Marmara Sea is 53 km, and is concentrated dominantly along the North Boundary and Central Marmara faults. The total offset is probably $\sim 80 \pm 10$ km. This figure is compatible with the other estimates of total offset along the North Anatolian Fault, which range between 25 and 85 km (e.g. Şengör, 1979; Barka, 1992). The total offset in the western Marmara Sea and along the Ganos Fault must be considerably less than 80 km, as this section of the North Anatolian Fault post-dates the TTT-triple junction phase. The 85 km of displacement inferred along the Ganos Fault by Armijo et al. (1999) is based on two stratigraphic–structural relations, which are not supported by detailed field observations (Yaltırak et al., 1999).

5.2. Timing

The North Anatolian Fault was initiated in the eastern Anatolia during the Late Miocene, and propagated westwards reaching the Marmara Sea region during the Pliocene (e.g. Şengör, 1979; Suzanne et al., 1990; Barka, 1992). The North Anatolian Fault must have been active in the İzmit Bay by the Late Pliocene, as shown by the sediments of this age recovered from the drill cores in the Bay (Meriç, 1995). A tighter age control on the propagation history of the North Anatolian Fault comes from the region of the Gallipoli Peninsula. Here, adjacent to the Ganos Fault, there is a continuous shallow marine to lagoonal sedimentary sequence (Gazhanedere, Kirazlı and Alçıtepe formations) of Mid-Miocene to Early Pliocene age, which shows no evidence of being deposited near a major fault (Görür et al., 1997b; Tüysüz et al., 1998; Yaltırak et al., 1998; Okay et al., 1999). This sequence is unconformably overlain in the Gallipoli Peninsula by Upper Pliocene coarse clastic rocks deposited in the footwall of a transpressive branch of the Ganos Fault (Tüysüz et al., 1998; Yaltırak et al., 1998). These stratigraphic data indicate that the North Anatolian Fault reached the region of the Gallipoli Peninsula by the mid-Pliocene; the fault reorganisation must have occurred shortly before, as shown by the Pliocene cover of the Terzili Fault Zone.

5.3. Kinematics

The North Anatolian Fault reached the İzmit Bay probably by the earliest Pliocene. It bifurcated

at the western boundary of the Bay, with the two branches being represented by the North Boundary–Terzili and the Biga faults (Fig. 16b). The creation of the northwestern and southwestern arms of the triple junction must have been coeval, since dextral strike-slip movement on the North Boundary–Terzili Fault or on the Biga Fault alone would have created a fault-bend basin or a major compressive ridge respectively, for which there is no geological evidence. Dextral strike-slip movement along the arms of the triple junction led to the opening of the Çınarcık Basin. At the mid-Pliocene there was a major fault reorganisation in the Marmara region, the Terzili Fault was largely abandoned, and the North Boundary Fault broke westward. Initially, it probably followed the shelf break of the northern Marmara shelf, then, with the creation of a major restraining fault bend, switched south to its present location. The Central Marmara Ridge started to rise as a fold belt in front of the restraining Central Marmara Fault segment, while the Çınarcık Basin continued its development, this time as a releasing fault-wedge basin between the North and Inner Boundary faults (Fig. 15).

5.4. The effect of the fault reorganisation on the basinal sedimentary sequences

The Çınarcık and North İmralı basins comprise two sequences distinguished mainly by their structural features. The lower sequence in the Çınarcık Basin is truncated by the basal parts of the North and Inner Boundary faults, and the upper sequence rests on these faults (Fig. 5). The lower sequence in the North İmralı Basin is folded and faulted, whereas the upper sequence is largely free of such deformation (Figs. 8, 12 and 13). It is probable that the unconformity between these sequences marks the period of the mid-Pliocene fault reorganisation in the Marmara region. Following the TTT-triple junction phase, the North and Inner Boundary faults are merging into a single fault plane from bottom upwards. The folding in the basinal sediments observed in the seismic section 29 (Fig. 7) is probably a result of the on-going convergence of the two faults.

The thickness of syn- and post-TTT-triple junction sequences in the Çınarcık and North İmralı basins can give a very rough estimate on the relative periods of these phases. The syn-TTT-triple junction sequences in both basins are 1.5 to 2 times thicker than post-TTT-triple junction sequences (cf. Figs. 5 and 8), which argues for a longer duration of the TTT-triple junction phase compared with the present strain regime.

6. Possible causes of bifurcation and subsequent reorganisation of the North Anatolian Fault

The Anatolian plate is translated westward along the 1200 km long North Anatolian Fault. For such a lithospheric displacement, a single fault zone is mechanically and energetically more favourable than two or more fault zones. The bifurcation of the North Anatolian Fault in the Marmara region must, therefore, have been due to unusual circumstances. It is suggested here that the westward-propagating North Anatolian Fault intersected at the western İzmit Bay a pre-existing major NW-trending fault, which guided its direction of propagation (Fig. 16a). This Palaeo-Terzili Fault formed the boundary between the Thrace Basin and the Strandja Massif during the Eocene to Miocene period (Fig. 2). The Strandja Massif consists of Palaeozoic and Mesozoic metamorphic and granitic rocks, which during the Tertiary formed a high between the Black Sea and the Thrace Basin. Along the western margin of the Strandja Massif, Middle Eocene–Oligocene neritic limestones lie unconformably over this crystalline basement and define the edge of the Thrace Basin. Southwestward the carbonates pass rapidly to several thousand metres of Eocene to Lower Miocene clastic sedimentary rocks. 20 km southwest of the shelf edge the thickness of the Eocene–Lower Miocene sequence exceeds 5000 m (Turgut et al., 1991). This rapid southwestward thickening of the Eocene–Lower Miocene sequence is achieved by growth faults along the future trend of the Terzili Fault (Turgut et al., 1991). The westward-propagating North Anatolian Fault intersected this Palaeo-Terzili Fault zone at the western İzmit Bay, and the Palaeo-Terzili Fault controlled the subsequent path of the North Anatolian Fault.

In contrast to the Terzili–North Boundary Fault, the Biga Fault does not correspond to a pre-existing weakness zone, at least in the section mapped on land. It is therefore not obvious why this southwestern arm of the triple junction was created. One possible reason may have been to avoid the formation of a very elongate fault-bend basin, which would have been created by the dextral motion along the North Boundary–Terzili Fault.

During the mid-Pliocene, the TTT-triple junction mechanism was abandoned and the North Anatolian Fault broke westward, initiating the present-day fault geometry in the Marmara Sea region (Fig. 16c). The Palaeo-Terzili Fault, which controlled the Eocene–Oligocene sedimentation in the Thrace Basin, becomes indistinct west of Edirne along with the termination of the Thrace Basin. Thus, when the North Boundary–Terzili Fault reached the terminus of the pre-existing weakness zone, it came across the crystalline rocks of the Rhodope and Strandja massifs, and the northwestward propagation became increasingly more difficult. This was probably the main reason for the mid-Pliocene fault reorganisation in the Marmara region.

7. Conclusions

The results of the present study, combined with that of Okay et al. (1999), show that the North Anatolian Fault under the Marmara Sea consists of a single major continuous fault zone, as recently suggested by Le Pichon et al. (1999) on the basis of historical seismicity. However, the 165 km long North Anatolian Fault under the Marmara Sea is not a single fault segment parallel to the GPS displacement vectors, as envisaged by Le Pichon et al. (1999), but is made up of four fault segments. The 15 km long Ganos segment in the extreme west forms the offshore continuation of the Ganos Fault with a strike of 57–68° (Okay et al., 1999). The Central Marmara segment between 27° 30′ and 28° 45′ is 105 km long and strikes 80–90°, whereas the 45-km-long North Boundary segment in the east has a strike of 107–119° (Fig. 2). At the entrance of the İzmit Bay, the North Boundary segment joins the east-trending İzmit segment, which was ruptured during the 17th August 1999 İzmit earthquake. The satellite laser ranging (SLR) studies indicate that the fault rupture in the İzmit segment dies out westwards towards the segment boundary with the North Boundary Fault. The North Boundary Fault may have been broken during an earthquake on 10.7.1894, which caused major damage in Istanbul (Ambraseys and Finkel, 1991). The 45-km-long onshore segment of the Ganos Fault and, most probably, its 15 km long offshore extension were ruptured during a major earthquake in 9.8.1912 (Ambraseys and Finkel, 1991). However, the Central Marmara segment has not ruptured since 1766 and, with the regional displacement vectors of ~20 mm/y, constitutes an imminent threat to the Marmara region.

This study also illustrates a new type of strike-slip basin that developed on the continental crust, a TTT-triple junction basin that has formed around an unstable triple junction of three dextral strike-slip faults. One important feature of this model is that the two arms of the triple junction are highly oblique to the regional displacement vector. In this particular case, the regional displacement vector has been east–west, whereas the two arms of the triple junction trend northwest and southwest respectively (Fig. 16), and it is the recognition of these oblique strike-slip fault segments on land that provides the strongest evidence for the TTT-triple junction origin of the Çınarcık Basin in the Sea of Marmara. The TTT-triple junction model shows that the opening of the Çınarcık Basin was achieved by pure dextral strike-slip faulting without requiring any regional north–south extension. An implication of this model is that, for periods of several million years, the brittle deformation in the continental crust can be modelled by rigid block translation with little internal deformation. A present-day example of rigid block translation of continental lithosphere is the motion of the Anatolian plate, as deduced from the seismicity and GPS measurements, which can be described by rigid body rotation around a pole in northern Egypt (e.g. Reilinger et al., 1997). The TTT-triple junction provides a piercing point to reconstruct the displacement history of the North Anatolian Fault, and indicates at least 53 km of

offset along the North Anatolian Fault in the eastern Marmara Sea. The TTT-triple junction model also provides an explanation for the origin of the transtensional North Boundary Fault segment, responsible for the on-going opening of the Çınarcık Basin. The origins of fault bends, junctions and transverse faults in strike-slip zones have been recurrent problems (e.g. Biddle and Christie-Blick, 1985). In this particular case this structure is a relic from an earlier fault geometry. The seismic sections indicate that the North Boundary Fault shows an anticlockwise rotation at depth to accommodate with the regional displacement vectors.

The westward propagation of the North Anatolian Fault in the Marmara region was controlled by a pre-existing, deep-seated fault zone, which led to its bifurcation during the Early Pliocene. The present active fault geometry was established subsequently during the mid-Pliocene, when the NW- and SW-trending arms of the North Anatolian Fault were largely abandoned. After the fault reorganisation, the Central Marmara Ridge started to form as a rising anticlinorium in front of the restraining Central Marmara Fault segment. Although the Central Marmara Fault has a fairly constant strike, it is transpressional in the west and transtensional in the east. This is based on the GPS displacement vectors showing an anticlockwise rotation of more than 7° between the two ends of the Central Marmara Fault (Straub et al., 1997).

The North Anatolian fault cannot be traced farther west than the North Aegean Trough, indicating a westward decrease in the offset of the North Anatolian Fault. This has been variously explained by a westward decrease in the slip rates along the North Anatolian Fault (Barka, 1992) or by a transfer of dextral displacement into the northeast extension in the North Aegean basins (Dinter and Royden, 1993). An alternative explanation is that most of the displacement of the North Anatolian Fault is distributed to several discordant splays in the Marmara region, so that the total dextral offset along the North Aegean trough is much less than that in the eastern Marmara Sea.

Acknowledgements

This study forms part of the National Marine Geology and Geophysics Programme (coordinator Naci Görür) supported by TÜBITAK grants YDABÇAG 198Y077 and 199Y079. We thank the Turkish Petroleum Company (TPAO) for access to the seismic sections in the Marmara region. Muzaffer Siyako is also thanked for inspiring discussions on the North Anatolian Fault. Nilgün Okay and Okan Tüysüz, and the journal referees H.-G. Kahle and Y. Mart provided helpful comments on the manuscript.

References

Akartuna, M., 1968. The geology of the Armutlu Peninsula in Turkish. İstanbul Üniversitesi, Fen Fakültesi Monografileri 20. 105 pp.

Ambraseys, N.N., Finkel, C.F., 1991. Long-term seismicity of Istanbul and of the Marmara Sea region. Terra Nova 3, 527–539.

Ambraseys, N.N., Finkel, C.F., 1995. Seismicity of Turkey and adjacent areas, a historical review, 1500–1800. Eren Yayıncılık, İstanbul, 244 pp.

Armijo, R., Meyer, B., Hubert, A., Barka, A., 1999. Westward propagation of the North Anatolian fault into the northern Aegean: timing and kinematics. Geology 27, 267–270.

Aydın, A., Nur, A., 1982. Evolution of pull-apart basins and their scale independence. Tectonics 1, 91–106.

Aydın, A., Schultz, R.A., Campagna, D., 1990. Fault-normal dilation in pull-apart basins: implications for the relationship between strike-slip faults and volcanic activity. Ann. Tecton. 4, 45–52.

Bargu, S., Sakınç, M., 1993. Structural features of the region between the İznik Lake and İzmit Bay. Yerbilimleri Dergisi 7, 45–76, (in Turkish).

Barka, A.A., 1992. The North Anatolian Fault Zone. Ann. Tecton. 6, 164–195.

Barka, A.A., 1997. Neotectonics of the Marmara region. In: Pfister, M. (Ed.), Active Tectonics of Northwest Anatolia — The Marmara Poly-Project. Hochschulverlag AG an der ETH, Zürich, pp. 55–87.

Barka, A.A., Kadinsky-Cade, K., 1988. Strike-slip fault geometry in Turkey and its influence on earthquake activity. Tectonics 7, 663–684.

Ben-Avraham, Z., Zoback, M.D., 1992. Transform-normal extension and asymmetric basins: An alternative to pull-apart models. Geology 20, 423–426.

Biddle, K.T., Christie-Blick, N., 1985. Strike-slip deformation, basin formation and sedimentation. Spec. Publ. Soc. Econ. Paleontol. Mineral. 37, 386 pp.

Chappell, J., Shackleton, N.J., 1986. Oxygen isotopes and sea level. Nature 324, 137–140.

Crampin, S., Evans, R., 1986. Neotectonics of the Marmara Sea region. J. Geol. Soc. London 143, 343–348.

Crowell, J.C., 1974. Origin of Late Cenozoic basins in southern California. In: Dickinson, W.R. (Ed.), Tectonics and Sedimentation. Soc. Econ. Paleontol. Mineral. Spec. Publ. 22, 190–204.

Crowell, J.C., 1979. The San Andreas fault system through time. J. Geol. Soc. London 136, 293–302.

Dinter, D.A., Royden, L., 1993. Late Cenozoic extension in northeastern Greece: Strymon Valley detachment system and Rhodope metamorphic core complex. Geology 21, 45–48.

Emre, Ö., Erkal, T., Tchepalyga, A., Kazancı, N., Keçer, M., Ünay, E., 1999. Neogene–Quaternary evolution of the eastern Marmara–Black Sea region, northwest Turkey. Maden Tetkik ve Arama Dergisi, in press, (in Turkish).

Ergün, M., Özel, E., 1995. Structural relationships between the Sea of Marmara basin and the North Anatolian Fault Zone. Terra Nova 7, 278–288.

Erguvanlı, K., 1949. Etude geologique de l'ile d'İmralı. Türkiye Jeoloji Kurumu Bülteni 2, 118–125.

Erinç, S., 1955. The marine Pleistocene deposits of Yalova. Türk Cografya Dergisi 2, 85–92, (in Turkish).

Görür, N., Okay, A.I., 1996. Fore-arc origin of the Thrace basin, northwest Turkey. Geol. Rund. 85, 662–668.

Görür, N., Monod, O., Okay, A.I., Şengör, A.M.C., Tüysüz, O., Yiğitbaş, E., Sakınç, M., Akkök, R., 1997a. Palaeogeographic and tectonic position of the Carboniferous rocks of the western Pontides (Turkey) in the frame of the Variscan belt. Bull. Soc. Géol. Fr. 168, 197–205.

Görür, N., Çağatay, M.N., Sakınç, M., Sümengen, M., Şentürk, K., Yaltırak, C., Tchapalyga, A., 1997b. Origin of the Sea of Marmara as deduced from Neogene to Quaternary paleogeographic evolution of its frame. Int. Geol. Rev. 39, 342–352.

Güneysu, A.C., 1998. Submarine and coastal geomorphology of the southern Marmara Sea. In: Studies on Marine Geology in Turkey, Workshop IV, 166–171.

Harding, T.P., 1985. Seismic characteristics and identification of negative flower structures, positive flower structures, and positive structural inversion. Am. Assoc. Petrol. Geol. Bull. 69, 582–600.

Ingersoll, R.V., Busby, C.J., 1995. Tectonics of sedimentary basins. In: Busby, C.J., Ingersoll, R.V. (Eds.), Tectonics of Sedimentary Basins. Blackwell, pp. 1–51.

Jackson, J., 1994. Active tectonics of the Aegean region. Annu. Rev. Earth Planet. Sci. 22, 239–271.

Keskin, C., 1974. The stratigraphy of the northern Ergene basin. In: Okay, H., Dileköz, E. (Eds.), Proceedings of the Second Petroleum Congress of Turkey. Association of the Turkish Petrolum Geologists, pp. 137–163.

Ketin, İ., 1953. Tektonische Untersuchungen auf den Prinzeninseln nahe İstanbul (Türkei). Geol. Rundsch. 41, 161–172.

Ketin, İ., Roesli, F., 1953. Makroseismische Untersuchungen über das nordwestanatolischen Beben vom 18. März 1953. Eclogae Geol. Helv. 46, 187–208.

Kopp, K.O., Pavoni, N., Schindler, C., 1969. Geologie Thrakiens IV: Das Ergene Becken. Beihefte Geol. Jahrbuch 76. 136 pp.

Le Pichon, X., Angelier, J., 1979. The Hellenic arc and trench system: a key to the neotectonic evolution of the Eastern Mediterranean area. Tectonophysics 60, 1–42.

Le Pichon, X., Taymaz, T., Şengör, A.M.C., 1999. The Marmara Fault and the future İstanbul earthquake. In: Karaca, M., Ural, D.N. (Eds.), Proceedings of the International Conference on the Kocaeli Earthquake, 17 August 1999. Istanbul Technical University Press House, Istanbul, pp. 41–54.

Mann, P., Hempton, M.R., Bradley, D.C., Burke, K., 1983. Development of pull-apart basins. J. Geol. 91, 529–554.

Marathon Oil Company, 1975. Marmara No. 1 well. Final well report, 26 pp.

May, S.R., Ehman, K.D., Gray, G.G., Crowell, J.C., 1993. A new angle on the tectonic evolution of the Ridge basin, a "strike-slip" basin in southern California. Geol. Soc. Am. Bull. 105, 1357–1372.

McKenzie, D.P., 1972. Active tectonics of the Mediterranean region. Geophys. J. R. Astron. Soc. 30, 109–185.

McKenzie, D.P., Morgan, W.J., 1969. Evolution of triple junctions. Nature 224, 125–133.

Meriç, E., 1995. Stratigraphy and depositional features of the Quaternary sequence in the Gulf of İzmit (Hersek Burnu–Kababurun). In: Meriç, E. (Ed.), Quaternary Sequence in the Gulf of İzmit. İstanbul, 251–258, (in Turkish).

MTA, 1964. Geological map, 1:500 000 scale, Istanbul sheet. Maden Tetkik ve Arama Enstitüsü, Ankara, Turkey.

Okay, A.I., Satır, M., Maluski, H., Siyako, M., Monie, P., Metzger, R., Akyüz, S., 1996. Paleo- and Neo-Tethyan events in northwest Turkey: geological and geochronological constraints. In: Yin, A., Harrison, M. (Eds.), Tectonic Evolution of Asia. Cambridge University Press, New York, pp. 420–441.

Okay, A.I., Demirbağ, E., Kurt, H., Okay, N., Kuşçu, İ., 1999. An active, deep marine strike-slip basin along the North Anatolian Fault in Turkey. Tectonics 18, 129–148.

Özhan, G., Bayrak, D., 1998. A seismic study of the Plio-Quaternary sediments in the İzmit Bay. Türkiye Jeoloji Bülteni 41, 151–164, (in Turkish).

Paluska, A., Poetsch, T., Bargu, S., 1989. Tectonics, paleoseismic activity and recent deformation mechanism in the Sapanca–Abant region (NW Turkey, North Anatolian Fault Zone). In: Zschau, J., Ergünay, O. (Eds.), Proceedings of the Turkish–German Earthquake Research Project, pp. 18–32.

Paton, S., 1992. Active normal faulting, drainage patterns and sedimentation in southwestern Turkey. J. Geol. Soc. London 149, 1031–1044.

Perinçek, D., 1991. Possible strand of the North Anatolian Fault in the Thrace Basin, Turkey — an interpretation. Am. Assoc. Petrol. Geol. Bull. 75, 241–257.

Pfannenstiel, M., 1944. Diluviale Geologie des Mittelmeerge-

bietes: die diluvialen Entwicklungstadien und die Urgeschichte von Dardanellen, Marmara Meer und Bosphorus. Geol. Rundsch. 34, 324–334.

Reilinger, R.E., McClusky, S.C., Oral, M.B., King, R.W., Toksoz, M.N., Barka, A.A., Kınık, I., Lenk, O., Şanlı, I., 1997. Global positioning system measurements of present-day crustal movements in the Arabia–Africa–Eurasia plate collision zone. J. Geophys. Res. 102, 9983–9999.

Rohr, K.M.M., Dietrich, J.R., 1992. Strike-slip tectonics and development of the Tertiary Quenn Charlotte basin, offshore western Canada: evidence from seismic reflection data. Basin Res. 4, 1–19.

Roussos, N., Lyssimachou, T., 1991. Structure of the central North Aegean Trough: an active strike-slip deformation zone. Basin Res. 3, 39–48.

Sakinç, M., Bargu, S., 1989. Stratigraphy of Late Pleistocene (Tyrrehenian) sediments in the Gulf of İzmit and neotectonics of the region. Türkiye Jeoloji Bülteni 32, 51–64, (in Turkish).

Şaroğlu, F., Emre, Ö., Kuşçu, I., 1992. Active Fault Map of Turkey. General Directorate of the Mineral Research and Exploration, Ankara, Turkey, 2 sheets, 1:2 000 000 scale.

Şengör, A.M.C., 1979. The North Anatolian transform fault: its age, offset and tectonic significance. J. Geol. Soc. London 136, 269–282.

Şengör, A.M.C., Görür, N., Şaroğlu, F., 1985. Strike-slip faulting and related basin formation in zones of tectonic escape: Turkey as a case study. In: Biddle, K.T., Christie-Blick, N. (Eds.), Strike-slip Deformation Basin Formation and Sedimentation. Soc. Econ. Paleontol. Mineral. Spec. Publ. 37, 227–264.

Şengör, A.M.C., Demirbağ, E., Tüysüuz, O., Kurt, H., Görür, N., Kuşçu, İ., 1999. A preliminary note on the structure of the Gulf of İzmit: implications for the westerly prolongation of the North Anatolian Fault. In: Karaca, M., Ural, D.N. (Eds.), Proceedings of the International Conference on the Kocaeli Earthquake, 17 August 1999. Istanbul Technical University Press House, Istanbul, pp. 25–37.

Seyir, Hidrografi ve Oşinografi Dairesi Başkanlığı, 1983. Bathymetric map of the Marmara Sea between Büyükçekmece and Hoşköy, scale 1:100 000 (Map No. 291).

Seyir, Hidrografi ve Oşinografi Dairesi Başkanlığı, 1987. Bathymetric map of the Marmara Sea, scale 1:300 000 (29 INT 3708).

Seyir, Hidrografi ve Oşinografi Dairesi Başkanlığı, 1989. Bathymetric map of the Marmara Sea south of Istanbul, scale 1:50 000 (INT 3754).

Sickenberg, O., Tobien, H., 1971. New Neogene and Lower Quaternary vertebrate faunas in Turkey. Newsl. Stratigr. 1, 51–61.

Siyako, M., Bürkan, K.A., Okay, A.I., 1989. Tertiary geology and hydrocarbon potential of the Biga and Gelibolu peninsulas. Bull. Turkish Assoc. Petrol. Geol. 1, 183–199, (in Turkish).

Smith, A.D., Taymaz, T., Oktay, F., Yüce, H., Alpar, B., Başaran, H., Jackson, J.A., Kara, S., Şimşek, M., 1995. High-resolution seismic profiling in the Sea of Marmara (northwest Turkey): Late Quaternary sedimentation and sea-level changes. Geol. Soc. Am. Bull. 107, 923–936.

Straub, C., Kahle, H.-G., 1995. Active crustal deformation in the Marmara Sea region, NW Anatolia, inferred from GPS measurements. Geophys. Res. Lett. 22, 2533–2536.

Straub, C., Kahle, H.-G., Schindler, C., 1997. GPS and geologic estimates of the tectonic activity in the Marmara region, NW Anatolia. J. Geophys. Res. 102, 27 587–27 601.

Suzanne, P., Lyberis, N., Chorowics, J., Nurlu, M., Yurur, T., Kasapoglu, E., 1990. La géométrie de la faille nord anatolienne à partir d'images Landsat-MSS. Bull. Soc. Géol. Fr. 6 (8), 589–599.

Sylvester, A.G., 1988. Strike-slip faults. Geol. Soc. Am. Bull. 100, 1666–1703.

Taymaz, T., Jackson, J., McKenzie, D., 1991. Active tectonics of the north and central Aegean Sea. Geophys. J. Int. 106, 433–490.

Turgut, S., Türkaslan, M., Perinçek, D., 1991. Evolution of the Thrace sedimentary basin and its hydrocarbon prospectivity. In: Spencer, A.M. (Ed.), Generation Accumulation and Production of Europe's Hydrocarbons. Spec. Publ. European Assoc. Petrol. Geoscientists vol. 1, 415–437.

Tüysüz, O., Barka, A., Yiğitbaş, E., 1998. Geology of the Saros Graben: its implications on the evolution of the North Anatolian Fault in the Ganos–Saros region, NW Turkey. Tectonophysics 293, 105–126.

Üçer, S.B., Crampin, S., Evans, R., Miler, A., Kafadar, N., 1985. The MARNET radiolinked seismometer network spanning the Marmara Sea and the seismicity of Western Turkey. Geophys. J. R. Astron. Soc. 83, 17–20.

Umut, M., 1988. Geological map and explanatory notes of the Kirklareli-C4 sheet scale 1:100 000. Maden Tetkik ve Arama Genel Müdürlüğü, Ankara.

USGS, 1999. National Earthquake Information Center — World Data Center for Seismology, Earthquake Bulletin, http://earthquake.usgs.gov.

Wong, H.K., Lüdmann, T., Uluğ, T.A., Görür, N., 1995. The Sea of Marmara: a plate boundary sea in an escape tectonic regime. Tectonophysics 244, 231–250.

Yaltırak, C., Alpar, B., Yüce, H., 1998. Tectonic elements controlling the evolution of the Gulf of Saros (northeastern Aegean Sea, Turkey). Tectonophysics 300, 227–248.

Yaltırak, C., Sakınç, M., Oktay, F.Y., 1999. Discussion to the paper by Armijo, R., Meyer, B., Hubert, A., Barka, A., 1999. Westward propagation of the North Anatolian fault into the northern Aegean: timing and kinematics. Geology 27, 267–270.

Yılmaz, Y., Genç, Ş.C., Yiğitbaş, E., Bozcu, M., Yılmaz, K., 1995. Geological evolution of the Late Mesozoic continental margin of nortwestern Anatolia. Tectonophysics 243, 155–172.